3. SITE 536[1]

Shipboard Scientific Party[2]

SITE 536

Date occupied: 0545 hr., 9 January 1981

Date departed: 1454 hr., 11 January 1981

Time on hole: 2 days, 9.15 hr.

Position: 23°29.39′N; 85°12.58′W

Water depth (sea level; corrected m, echo-sounding): 2790

Water depth (rig floor; corrected m, echo-sounding): 2800

Bottom felt (m, drill pipe): 2808.5

Penetration (m): 213

Number of cores: 23

Total length of cored section (m): 213

Total core recovered (m): 65.73

Core recovery (%): 31

Oldest sediment cored:
Depth sub-bottom (m): 213
Nature: Dolomite
Age: Unknown
Measured velocity (km/s): 6.12

Basement: Not penetrated

Principal results: See Summary section.

SUMMARY

Site 536 was the first of three short holes to be drilled into high-standing basement blocks. The site is located on a submarine ridge at the base of the Campeche Escarpment. Although the hole had to be abandoned because of unstable hole conditions before definitive basement was reached, an interesting Tertiary-Mesozoic sequence with diverse lithologies was recovered. The location of Site 536 is shown on Figure 1, and the drilling results are summarized below and in Figure 2.

Three major lithologic subdivisions were drilled as follows.

1. foraminiferal-nannofossil ooze and chalk (0–80 m)—Pleistocene to Late Cretaceous (late Maestrichtian) (Units I–II)
2. limestone with neritic and planktonic material (80–188.5 m)—Early Cretaceous (Aptian-Albian) (Unit III)
3. dolomite (188.5–213 m)—age unknown (Unit IV)

These rocks represent very different episodes in the history of the area.

The Upper Cretaceous and Tertiary pelagic section is punctuated with numerous hiatuses, but a complete record of the Cretaceous/Tertiary boundary is preserved. There is little indication that the Campeche platform shed significant coarse debris in the Late Cretaceous or Cenozoic, supporting the notion that the platform "stepped back" and abandoned a steep margin during the mid-Cretaceous. The site remained a deep-water, pelagic environment throughout the Late Cretaceous-Cenozoic.

The Lower Cretaceous limestones are composed of sand and rubble-size debris of rudists, corals, algae, and other shallow-water material from the margin of a platform. Pelagic nannofossil chalk with radiolarians and foraminifers is interbedded with this debris and occasionally fills voids in rudists. Age of the plankton increases downward from Albian to late Aptian. The neritic debris accumulated over considerable time as talus at the foot of a Cretaceous platform slope that was probably located at the site of the present-day Campeche Escarpment, 5 km to the west. Similar talus aprons have been reported from the foot of the Golden Lane platform (Poza Rica belt) in Mexico. Like the Poza Rica rocks, the talus deposits at Site 536 are highly porous, in part because of selective leaching of aragonite shells *in situ*.

The basal dolomite was probably deposited on a shallow-water platform. Diagenesis has erased most of the primary features, but it preserved some crinkled algal laminations, probable desiccation cracks, and intraclasts that suggest intertidal to supratidal conditions, alternating with shallow-marine episodes represented by layers of skeletal debris (mostly represented by molds). The tight fabric with porosities as low as 1% and sonic velocities over 6 km/s possibly indicate considerable burial diagenesis. The induration and depositional environment of the dolomite contrast sharply with the overlying Lower Cretaceous limestones, which contain only material from a platform margin, are highly porous, and show few signs of burial diagenesis. The dolomite may be part of a Jurassic carbonate underpinning of the high-rising Cretaceous platforms. Seismic stratigraphy

[1] Buffler, R. T., Schlager, W., et al., *Init. Repts. DSDP*, 77: Washington (U.S. Govt. Printing Office).

[2] Richard T. Buffler (Co-chief Scientist), Institute for Geophysics (formerly Marine Science Institute), The University of Texas at Austin, Austin, Texas; Wolfgang Schlager (Co-Chief Scientist), School of Marine and Atmospheric Science, University of Miami, Miami, Florida (present address: University of Miami, 4600 Rickenbacker Causeway, Miami, Florida 33149); Jay L. Bowdler, Union Oil Company of California, Houston, Texas; Pierre H. Cotillon, Département de Géologie, Université Claude Bernard, 69622 Villeurbanne Cedex, France; Robert B. Halley, Branch of Oil and Gas Resources, U.S. Geological Survey, Denver, Colorado; Hajimu Kinoshita, Department of Geophysics, Chiba University, Chiba 260, Japan; Leslie B. Magoon III, U.S. Geological Survey, Menlo Park, California (present address: U.S. Geological Survey, 3475 Deer Creek Road, Palo Alto, California 94304); Charles L. McNulty, Department of Geology, University of Texas at Arlington, Arlington, Texas; James W. Patton, Marathon Oil Company, Littleton, Colorado; Kenneth A. Pisciotto, Scripps Institution of Oceanography, University of California at San Diego, La Jolla, California (present address: Sohio Petroleum, 50 Fremont Street, San Francisco, California 94105); Isabella Premoli Silva, Istituto di Paleontologia, Università di Milano, Milano, Italy; Otmara Avello Suarez, Oceanological Institute, Havana, Cuba; Margaret M. Testarmata, Institute for Geophysics (formerly Marine Science Institute), The University of Texas at Austin, Austin, Texas; Richard V. Tyson, School of Environmental Sciences, University of East Anglia, Norwich NR4 7TJ, United Kingdom; David K. Watkins, Department of Geology, Florida State University, Tallahassee, Florida.

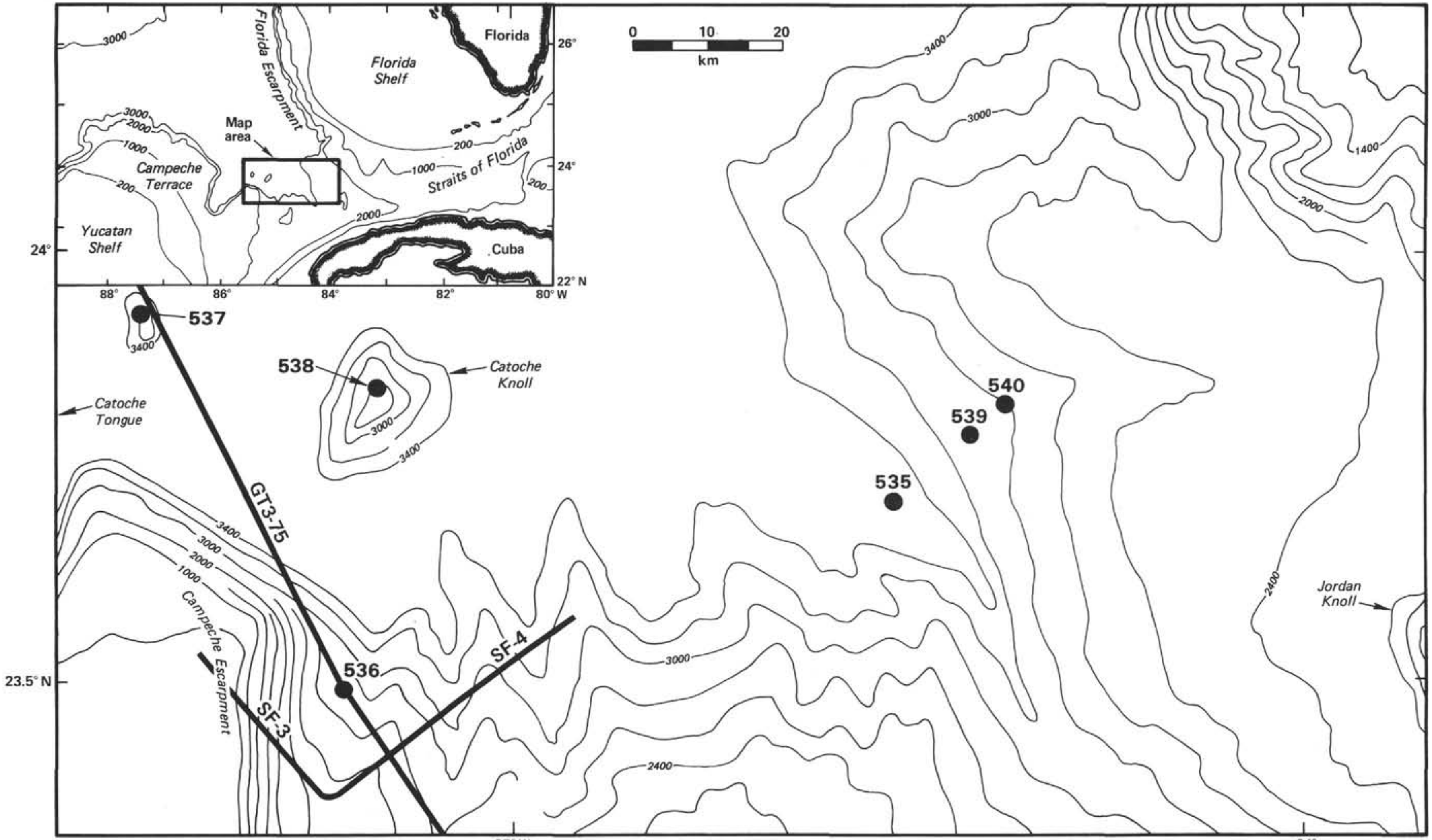

Figure 1. Location map of Leg 77 sites, western Straits of Florida.

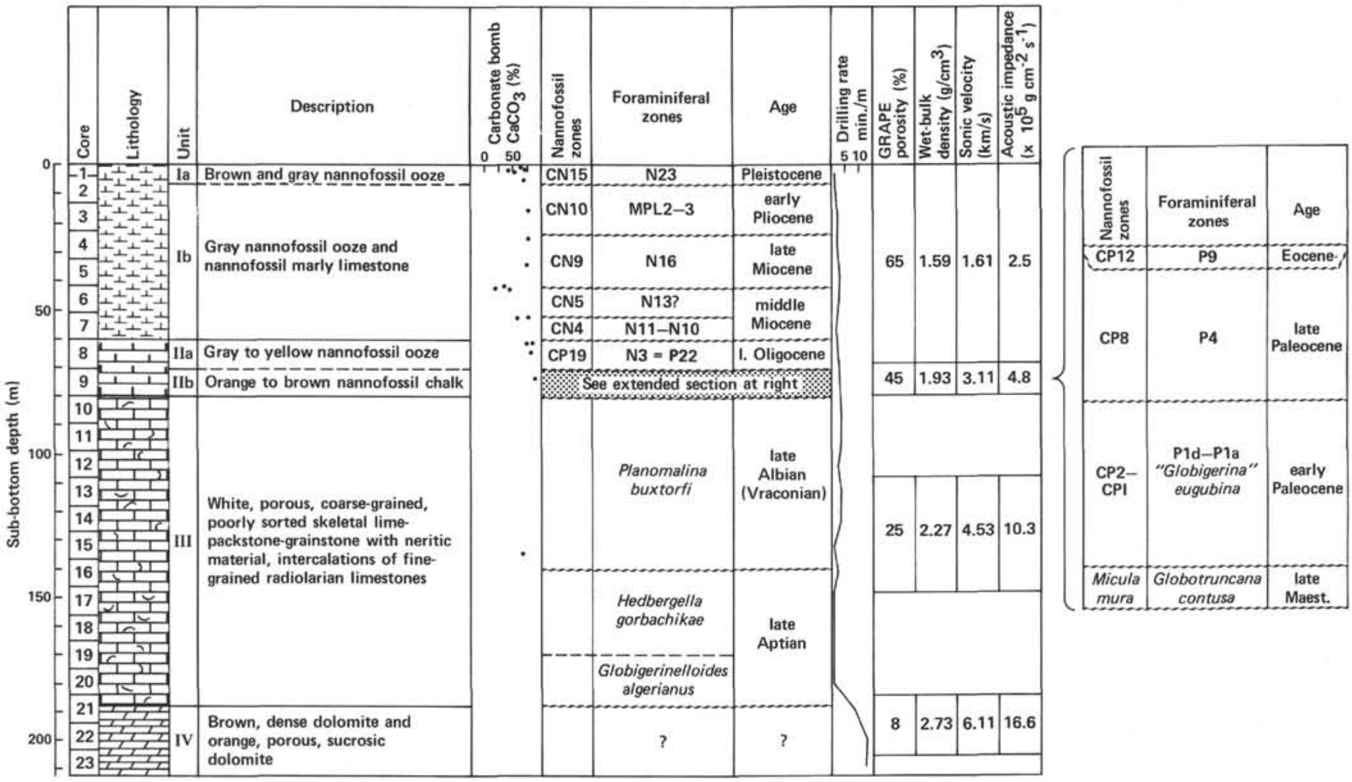

Figure 2. Stratigraphic summary of Hole 536. See Introduction and Explanatory Notes chapter for lithology symbols.

supports this view. However, we cannot exclude the possibility that the rock is part of a completely different sedimentary cycle and is Paleozoic in age.

BACKGROUND AND OBJECTIVES

Site 536 was one of several sites designed to test basement in the southeastern Gulf of Mexico in order to provide clues to its nature, age, and origin. These sites were located in an area where inferred basement blocks occur near the seafloor and have only a thin (200–300 m) sedimentary cover. This area occurs along the western part of the deep southeastern Gulf just northeast of the Campeche Escarpment in the vicinity of Catoche Knoll (Fig. 1). A more general discussion of the background and objectives of the basement sites is contained in Introduction and Explanatory Notes chapter (this volume) and in the site chapter for Site 537 (this volume). Unfortunately, basement was not reached at Site 536 because of drilling problems.

Site 536 is located along the base of the Campeche Escarpment in an area of irregular seafloor topography that stands above the general level of the flat-lying abyssal Gulf plain to the north (Fig. 1). The area is scoured by northwest-southeast trending channels that may be, in part, structurally controlled.

Seismic Line GT3-75 (Fig. 3) shows the interpreted geologic setting that was to be drilled. The chosen site included an inferred high-standing basement block overlain by a relatively thin cover of sediment (Fig. 3). A strong reflector or acoustic basement at about 4 s, inferred to represent the top of a large basement block, was the primary objective of the hole. Another prominent reflector midway in the section represents a major unconformity of inferred mid-Cretaceous age. The thin, relatively transparent sequence above this unconformity was thought to represent mainly Tertiary oozes and chalks, based on correlation of seismic data with previous drilling in the area (Sites 96 and 97, Worzel, Bryant, et al., 1973). The section below the unconformity is inferred to represent the updip part of a thick Mesozoic sedimentary sequence seen on the seismic data further to the south and east (Fig. 3). A prominent unconformity underlying the inferred Mesozoic rocks truncates an older rift sequence, which may possibly represent an earlier Triassic–Early Jurassic rift basin (Fig. 3). Drilling these sedimentary sequences above basement was an important secondary objective of this site, because data from these sequences could provide important clues to the early tectonic and sedimentary history of the region.

OPERATIONS

Glomar Challenger left Site 535 at 2330 hr. on 8 January for Site ENA-14C (the future Site 536). The 3.5-kHz and 12-kHz bottom profilers and two airguns were run underway. The ship approached the site on course 305°, duplicating seismic Line GT3-75 (Figs. 1, 3). Topography in the vicinity of the site consists of a steeply northeast-dipping, gullied slope at the foot of the Campeche Escarpment with variable cover of soft sediment (Figs. 1, 3). After dropping a 13.5-kHz beacon at the designated Site ENA-14C at 0545 hr., 9 January, the ship made two loops over the site to reconnoiter the topography. At 0806 hr., the ship was in final position in 2808.5 m water depth. By 1730 hr., a new sand line had

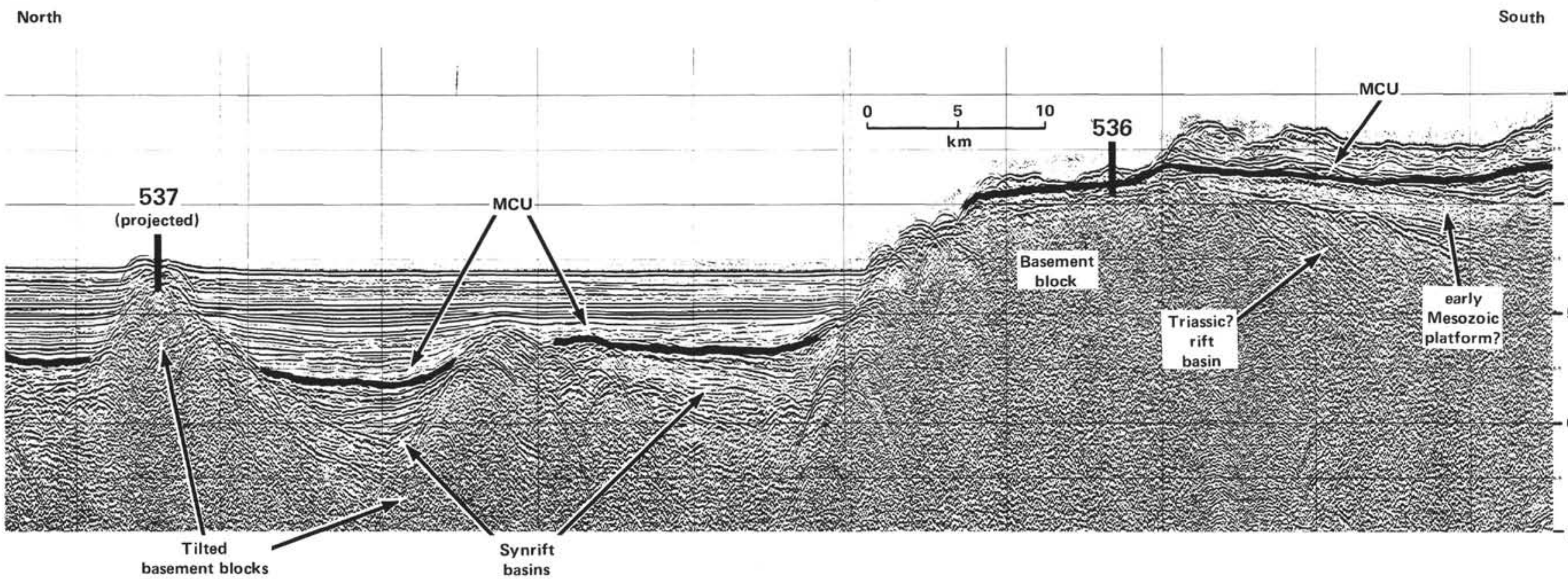

Figure 3. Regional seismic Line GT3-75 showing geologic setting of Sites 536 and 537. See Figure 1 for location of line. MCU = mid-Cretaceous unconformity.

been spooled on and a new bottom-hole assembly made up with a F94CK bit. Site 536 was spudded at 2220 hr., 9 January. We cored continuously through Cenozoic firm ooze (Table 1). Two heat flow measurements at 2860 and 2888 m were successful, but both times either the ooze was too stiff to yield interstitial water samples or the sampling mechanism failed. Cretaceous limestones containing coarse, shallow-water debris were penetrated from 80–184 m (Table 1). They were poorly cemented and fast to drill, but loose pieces would fall in the hole and jam the pipe. In spite of flushing with guar, the drill string was stuck several times and recovery dropped to 4% (Table 1). The last three cores were taken in hard, sucrosic dolomite. Recovery in this unit was better, but hole conditions deteriorated because of the rocks falling in from the overlying limestones. On 11 January morning, because of the increasing hazard to the drill string, we decided to pull out of the hole and abandon the site. There was no indication that the zone of rubbly limestone could be avoided by offsetting and drilling another hole nearby. By 1454 hr., the bit was on deck and the ship underway for Site 537. Total depth reached was 213 m, and time on site was 2 days, 9 hr. Only minor currents were observed while on station.

SEDIMENTOLOGY

We divided the sediment sequence recovered at Site 536 into four units. Top to bottom, these units are ooze, ooze and chalk, limestone, and dolomite. Both ooze and ooze and chalk units were further subdivided into subunits based on more subtle variations of color and clay content. Generally, these subunits separate more clay-rich, brown and orange lithologies from gray and greenish ooze and chalk. The units and subunits are illustrated graphically in Figure 2 and listed in Table 2.

Unit I: 0–61 m, Cores 1–7, Holocene-Miocene

The unit consists predominantly of very light gray nannofossil ooze. Lithification increases toward the base

Table 1. Coring summary, Hole 536.

Core	Date (Jan. 1981)	Time	Depth from drill floor (m)	Depth below seafloor (m)	Length cored (m)	Length recovered (m)	Percent recovery
1	9	2310	2808.5–2812.5	0.0–4.0	4.0	3.95	99
2	10	0022	2812.5–2822.0	4.0–13.5	9.5	3.20	34
3	10	0127	2822.0–2831.5	13.5–23.0	9.5	8.57	90
4	10	0231	2831.5–2841.0	23.0–32.5	9.5	9.05	95
5	10	0337	2841.0–2850.5	32.5–42.0	9.5	3.15	33
6	10	0441	2850.5–2860.0	42.0–51.5	9.5	2.13	22
7	10	0737	2860.0–2869.5	51.5–61.0	9.5	5.28	56
8	10	0839	2869.5–2879.0	61.0–70.5	9.5	7.24	76
9	10	0947	2879.0–2888.5	70.5–80.0	9.5	7.89	83
10	10	1251	2888.5–2898.0	80.0–89.5	9.5	0.60	6
11	10	1413	2898.0–2907.5	89.5–99.0	9.5	0.20	2
12	10	1518	2907.5–2917.0	99.0–108.5	9.5	0.10	1
13	10	1637	2917.0–2926.5	108.5–118.0	9.5	0.54	6
14	10	1753	2926.5–2936.0	188.0–127.5	9.5	0.78	8
15	10	1853	2936.0–2945.5	127.5–137.0	9.5	0.30	3
16	10	2001	2945.5–2955.0	137.0–146.5	9.5	0.55	6
17	10	2102	2955.0–2964.5	146.5–156.0	9.5	0.30	3
18	10	2205	2964.5–2974.0	156.0–165.5	9.5	0.37	4
19	10	2259	2974.0–2983.5	165.5–175.0	9.5	0.22	2
20	11	0002	2983.5–2993.0	175.0–184.5	9.5	0.20	2
21	11	0211	2993.0–3002.5	184.5–194.0	9.5	2.63	28
22	11	0517	3002.5–3012.0	194.0–203.5	9.5	3.56	37
23	11	0939	3012.0–3021.5	203.5–213.0	9.5	4.92	52
					213.0	65.73	31

Table 2. Summary of lithologic units at Hole 536.

Lithologic units or subunits	Sub-bottom depth (m)	Cores[a]	Age
Ia	0–4.5	1–2 (55 cm)	Holocene-Pleistocene
Ib	4.5–61	2 (55 cm)–7	Pleistocene-Miocene
IIa	61–70.5	8	Miocene-Oligocene
IIb	70.5–80	9	Eocene-Maestrichtian
III	80–188.5	10–21 (4 m)	Albian-Aptian
IV	188.5–213	21 (4 m)–23	pre-Aptian

[a] Measurements in parentheses are depths in the core: 2(55 cm) means 55 cm into Core 536-2.

of the unit and thin, deformed, soft chalk intervals are common in Cores 6 and 7. Within Unit I, two subunits (a and b) are distinguished on the basis of color and clay content.

Subunit Ia. This subunit (0.0–4.5 m) is a moderate yellowish brown, pale yellowish brown, light brownish gray foraminiferal-nannofossil ooze, with lesser amounts of very light gray, light gray, light olive gray, and medium gray nannofossil ooze. These sediments contain 30–80% nannofossils, 5–30% planktonic foraminifers, 10–75% clay, 5–10% diatoms, and a few percent each of mica, glauconite, quartz, sponge spicules, tunicate spicules, fish debris, and silicoflagellates. Three greenish glauconitic layers, each less than 5 mm thick, occur in the subunit, one at 76 cm and two at 190 cm in Core 1. Variations in clay content are responsible for the remainder of the color contrast observed in the subunit. All primary sedimentary structures are greatly distorted by drilling.

Subunit Ib. This subunit (4.5–61.0 m) is a light gray, very light gray, light greenish gray, and light olive gray nannofossil ooze. Greenish gray and yellowish gray colors are common in clayey intervals, particularly in Core 6, which contains intervals of nannofossil marl. The composition of this subunit ranges from 35–87% nannofossils, 5–13% foraminifers, 2–80% clay, 0–15% diatoms, and minor (less than 5%) amounts of glauconite, dolomite, quartz, pyrite, volcanic glass, sponge spicules, and silicoflagellates. The core was deformed during drilling. Streaks and deformed burrows of darker ooze are common and usually more clayey than the surrounding matrix. These streaks and burrows are yellowish gray, grayish green, light olive gray, and dark gray. Pyritized burrows occur in Core 4 and, in general, there is more pyrite in this subunit than the one above. Core 6 contains more clay; it includes two intervals of nannofossil clay in Section 536-6-1. The base of Subunit Ib (the boundary between Units I and II) is taken between the base of Core 7 and a distinctive medium gray nannofossil ooze occurring at the top of Core 8.

Unit II: 61–80 m, Cores 8–9, Miocene-Maestrichtian

This unit encompasses the diagenetic transition of soft ooze to firm chalk and is primarily a soft, nannofossil chalk with thin layers of ooze at scattered intervals throughout the cores. Core 8 is dominantly ooze; Core 9 is mostly chalk. We subdivided the unit into two parts, generally separating orange and brown lithologies from gray and green ones.

Subunit IIa. This subunit (Core 8) is dominantly yellowish gray to white nannofossil ooze. Glauconite and pyrite occur as small grains throughout, and indistinct clay-rich bands occur at intervals of about 20–50 cm in the core. Other minor constituents include foraminifers (3–10%) and radiolarians (less than 5%).

Subunit IIb. This subunit (Core 9) begins with a 15-cm-thick, white limestone and yellow brown chert layer at the top of the core. The chert is composed of opal CT and quartz. The bulk of the subunit is grayish orange, mottled grayish orange pink, and pale orange foraminiferal-nannofossil chalk with yellowish brown mottles. The mottles and streaks contain up to 85% clay. Medium gray patches of finely divided pyrite are common. Other minor constituents include dolomite, quartz, feldspar, tunicate spicules, and calcispheres. At the base of the subunit is a 40-cm-thick greenish, variably lithified calcareous interval containing foraminifers, micritic peloids, clay, and sphere-shaped grains (possibly foraminifer chamber fills and replacements and/or volcanic glass). Lesser amounts of radiolarians, nannofossils, and glauconite also occur. This interval is graded, plane-laminated, and cross-laminated; it may represent a turbidite.

Units I and II represent a pelagic sequence, punctuated by long periods of nondeposition and/or erosion. Turbidites and related sediments are essentially absent from the Tertiary section at this site. The possible turbidite at the base of Core 9 is of Late Cretaceous age. Although there is some drilling disturbance, Section 536-9-5 shows no significant lithologic variation across the Cretaceous/Tertiary boundary at about 70–71 cm (Fig. 4).

Unit III: 80–188.5 m, Cores 10–21, Albian-Aptian

Unit III is white limestone. Recovery was particularly poor in this interval (about 4%). Two types of limestone were recovered as drilling breccia; about 25% of the recovered pieces were large enough not to have been rotated in the core liner (Fig. 5). The first type, encountered in Cores 10 to 13 is a coarse-grained to medium-grained limestone. The material varies from well-sorted, medium-grained grainstones to very poorly sorted limestones with individual clasts up to 5 cm in length (Fig. 5A). The second limestone type consists of irregular, finer-grained wackestone and packstone horizons that contain planktonic foraminifers and radiolarians (Fig. 5B). The coarse material of these limestones consists of fragments of rudists, gastropods and other molluscs, corals, echinoderms, bryozoans, dasycladacean and codiacian (green calcareous) algae, coralline (red calcareous) algae, and a few benthic foraminifers. Foraminiferal-radiolarian wackestones occur in Core 14. Several pieces of limestone in this core display bedding in the form of wackestone layers, 1–2 cm thick, with apparent(?) dip between 30 and 45° (Fig. 5B).

In the remaining cores of this unit, at least nine intervals of fine-grained limestones (mudstone) were recovered, all separated by coarser limestone (grainstone). The fine-grained rocks are of several different ages and range from late Albian (but not latest Albian) to late

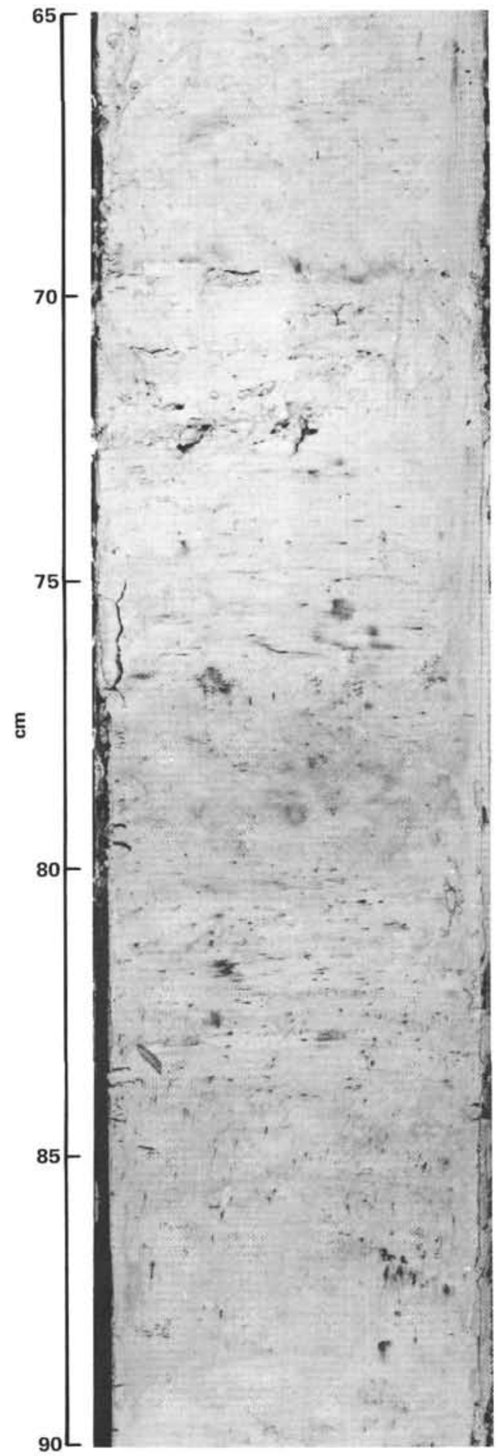

Figure 4. Core section (536-9-5, 65–90 cm) containing the Cretaceous/Tertiary boundary at 536-9-5, 70–71 cm.

Aptian. A sample of fine-grained limestone recovered from Core 18 contains a prominent, 1-cm-thick grainstone layer composed of shallow-water skeletal debris.

In both hand specimen (Fig. 6) and thin section, it is apparent that the grainstones have been leached. Most of the originally aragonitic skeletal material in these sediments has been dissolved to leave secondary pores.

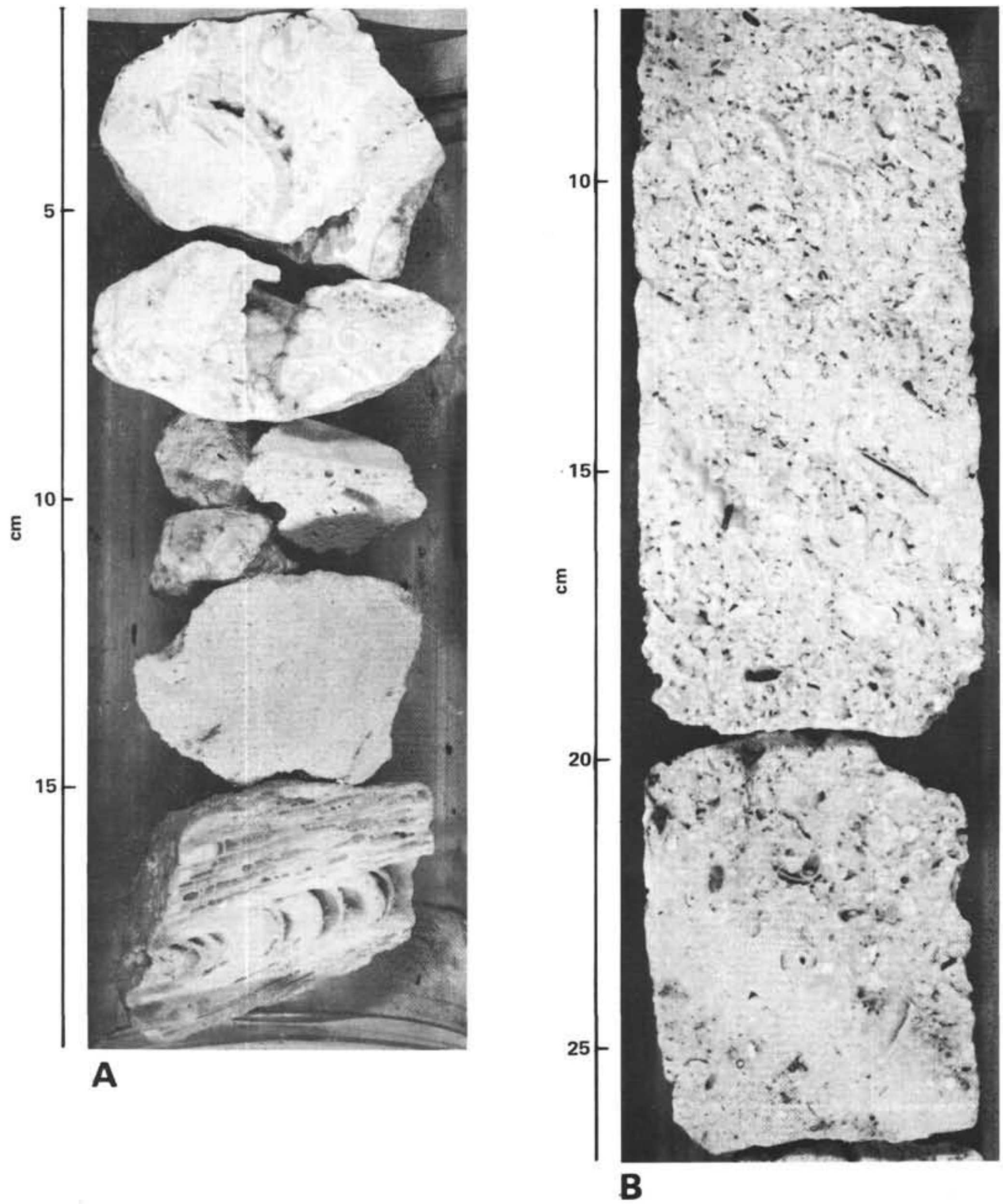

Figure 5. Representative intervals of limestones in Unit III at Site 536. A. Medium-grained to coarse-grained grainstones showing skeletal debris, variable porosity, and mode of recovery (536-11-1, 0–20 cm). B. Steeply dipping, skeletal grainstones of Unit III (536-14-1, 7–27 cm). (Note different cm scales.)

The remainder of the aragonite has been replaced by calcite, resulting in a rock with a total porosity as high as 50%.

Calcite cement is widespread in all grainstones. It occurs as an even coating of 5–15-μm crystals of scalenohedral calcite lining both primary and secondary pores. Most secondary pores are outlined by a delicate rim of micrite and cement a few tens of microns wide, the "micrite envelopes" of carbonate petrographers. They are not broken or distorted in any way, indicating that leaching of aragonite probably occurred while these sediments were in their present location.

The fine-grained and coarse-grained limestones of Unit III probably represent pelagic and bank margin limestones, respectively. The association of such sediments suggests that the shallow-water component is allochthonous, shed down a slope into deeper-water environments where it could mix and be interlayered with pelagic limestones. This interpretation is supported by the presence of single core pieces containing both pelagic and bank facies sediments. Contacts between the two facies encountered in some core pieces may indicate true depositional dips.

The presence of redeposited sediments at this site is consistent with its position close to the Cretaceous shelf edge. Unit III is encountered approximately 1000 m below and about 15 km east of the crest of the Albian reef (generally taken to be the top of the Campeche Escarpment; Worzel, Bryant, et al., 1973). Unit III is less than 5 km from the base of the Campeche Escarpment, sug-

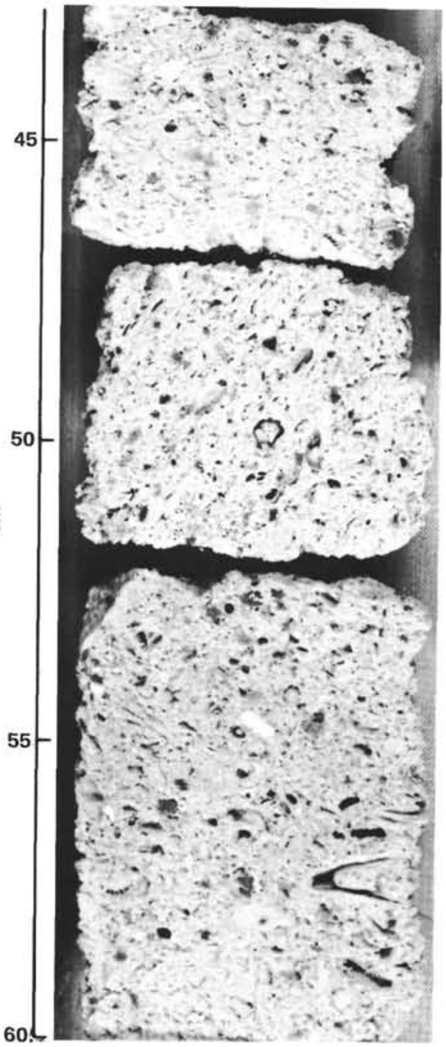

Figure 6. Grainstone showing well-developed secondary porosity (536-10-1, 43–60 cm).

gesting that this material could easily be a major accumulation of shallow-water debris that has been transported to oceanic depths.

Unit IV: 188.5–213 m, Cores 21–23, pre-Aptian

Unit IV consists of dense, brown, fine-grained to medium-grained dolomite. Because it is considerably harder than the overlying lithology and drilled much more slowly, the driller could identify the top of this unit at about 4 m into Core 21. Recovery of this unit averages 39%. Pieces of white limestone (skeletal grainstone) identical to the overlying unit occur 15 cm below the top of this unit. Drillers report a drop in the drill string and a loss of circulation at this point, suggesting that they encountered a void partly filled with sediment from Unit III.

Four distinct types of dolomite are differentiated in Unit IV based on color, texture, and relict sedimentary structures. These dolomites are probably massive replacements of preexisting carbonates. In thin section, the rocks are composed of dolomite rhombs and interlocking grains averaging 5-10 μm in fine-grained dolomites and 60–100 μm in medium-grained "sucrosic" dolomites. Scattered quartz grains occur in some thin sections. Clay fills many interstices between dolomite grains and imparts a variety of shades of brown and orange to the rock. Typical colors are dark yellowish brown, light yellowish brown, reddish yellow, and dark yellowish orange.

Of the four dolomite types recognized in Unit IV, the most common is Type 1, fine-grained, homogeneous, dark brown, and massive (Fig. 7A). It breaks with a conchoidal fracture and is slightly siliceous. Irregular vugs up to 1.5 cm in diameter occur sporadically in this lithology resembling voids left by leached nodular anhydrite. They are commonly filled with soft greenish clay containing isolated dolomite rhombs.

Type 2 dolomite (Fig. 7B) is similar to the first variety but clearly burrow mottled. Individual burrows are up to 2 cm in diameter and generally lighter in color and more coarse-grained than the surrounding matrix.

Type 3 dolomite is vaguely to distinctly laminated or banded and includes apparent intraformational breccias and clasts. Individual laminae are usually irregular and cracked; some have a crinkled appearance (Fig. 7C), whereas others occur in lithoclasts. Laminations and lithoclasts differ in both texture and color from their surrounding matrix because of different dolomite grain size and different amounts of clay (palygorskite?). One occurrence of fenestral (bird's-eye) vugs was noted in this facies. These are small (1–5 mm) elongate voids parallel to the rock lamination (Fig. 7A).

Type 4 dolomite is orange to brown, medium-grained, and "sucrosic" dolomite (Fig. 7D). Pores are common, some of which are mollusc molds, in particular gastropods and pelecypods. Porosity is highest in this type of dolomite (about 15%); the other types rarely have more than 2% (except for the "bird's-eye" and solution vug dolomites).

The four dolomite types are intercalated throughout the 11 m recovered: Type 1 occurs 12 times; Type 2, 10 times; Type 3, 8 times; and Type 4, 11 times. The individual dolomite types rarely exceed 50 cm and average about 20 cm.

These rocks are interpreted to be dolomitized, shallow subtidal to supratidal carbonates, characteristic lithologies of interior carbonate platforms. The most diagnostic of these rocks are the Type 3 dolomites. Laminated portions are directly comparable to algal laminations in tidal flat sediments, complete with fenestral (bird's-eye) desiccation features and laminae disruption. Some laminae are brecciated and dislocated by exposure and weathering. Thicker breccias (interpreted to be storm layers) are also present.

The other dolomite types probably represent dolomitized equivalents of: fine-grained lagoonal, and perhaps hypersaline, mudstone (Type 1); burrowed, more normal, marine subtidal and intertidal mudstone (Type 2); and thin concentrations of skeletal material forming packstones, wackestones, and grainstones, perhaps as tidal channel lag accumulations or low-energy beach deposits (Type 4). The alternation of these lithologies is typical for thick platform-interior carbonate sequences.

BIOSTRATIGRAPHY

Summary

The fossil content of the four lithologic units at this site varies widely in both abundance and composition. The first two units, pelagic and biogenic in origin, are characterized by rich, generally well-preserved planktonic faunas and floras, which range in age from Holocene–late Pleistocene through latest Cretaceous (Cores 1 through 9). The high biostratigraphic resolution with foraminifers and nannofossils in this time span revealed that large portions of the Tertiary sediments are missing in the recovered sequence at this site. The sedimentary expression of hiatuses varies from more common simple unconformities, neatly marked by changes in color or composition of the lithotypes, to obvious hardgrounds with dark crusts enriched in manganese.

The sequence of events for the first two units can be summarized as follows (from top to bottom) (Fig. 2).

Core 536-1 to Section 536-2-2: Holocene to late Pleistocene (CN15; N23)

Hiatus of approximately 4 Ma, corresponding to most of the Pleistocene through late Pliocene and late early Pliocene (CN14 through CN10; N22 through MPL3).

Level 536-2-2, 140 cm through Core 536-3: early Pliocene (CN10; MPL2)

Hiatus of about 3 Ma, corresponding to the earliest Pliocene and most of the late Miocene (CN10 through CN8; MPL1 through late N16).

Cores 536-4 and 536-5: early late Miocene (early Tortonian) (CN9; middle and early N16)

Hiatus of 4.5 Ma, very low rate of deposition for about 2 Ma, corresponding to the earliest late Miocene through late middle Miocene (CN8 through CN6; earliest N16 through N14). (Poor recovery in Cores 5 and 6 prevents confirmation of one or the other hypothesis.)

Core 536-6: late middle Miocene (CN5; possibly N13)

Hiatus of about 0.8 Ma, corresponding to middle Miocene (N13 [partim]? through late N11).

Cores 536-7 to level 536-8-1, 7 cm: early middle Miocene (late CN4; early N11 to N10)

Hiatus of about 11 Ma, corresponding to the remainder of the middle and early Miocene and to latest Oligocene (early late CN4 through CN1; N9 through N4).

Level 536-8-1, 8 cm to 536-8,CC: late Oligocene (CP19; N3 = P22)

Hiatus of about 26 Ma, corresponding to the remainder of the Oligocene and to late and middle Eocene (CP18 through CP12 [partim]; P21 through P10).

Interval 536-9-1, 0–2 cm: late early Eocene (CP12; late P9)

Hiatus of about 6.5 Ma, marked by a thin hardground, corresponding to the remainder of the early Eocene and to the latest Paleocene (CP11 through CP8b; early P9 through P5).

Levels 536-9-1, 3 cm through 536-9-3, 20 cm: middle late Paleocene (CP8; late P4)

Hiatus of about 4.5 Ma, corresponding to the early late and late early Paleocene (CP7 through CP3; P3 through P2)

Levels 536-9-3, 21 cm through 536-9-5, 69 cm: middle early to earliest Paleocene (CP2 through CP1; P1d through P1a; "*Globigerina*" *eugubina* Zone).

Levels 536-9-5, 95–96 cm through 536-9,CC: late Maestrichtian (*Micula mura* Zone; *Globotruncana contusa* Zone). Although this interval can be reliably assigned on the basis of both fossil groups to the late Maestrichtian, several critical forms of the *Abathomphalus mayaroensis* foraminiferal Zone were not seen. The sedimentary structures in this interval suggest a turbidite origin. Thus erosion and/or redeposition may account for the missing forms.

In summary, at Site 536 the total duration of deposition during the Cenozoic adds up to less than 10 Ma, or less than 15% of the total length of the Cenozoic (calculated to be about 65 Ma). Remarkably enough, about one-third of the depositional time at Site 536 is represented by lower Paleocene sediments, whose recovery is particularly striking for a location characterized by so many large hiatuses. Typically, lower Paleocene sediments are missing or are quite incomplete at deep-sea sites.

The third unit, a carbonate sequence of limestones containing shallow-water skeletal debris alternating with pelagic limestones (Core 536-10 through 536-21-1, 34 cm), is much older than the overlying Unit II. The occurrence of some planktonic foraminifers in the pelagic limestone dates the top of this unit as latest Albian (= Vraconian) separated by a hiatus of about 35 Ma from the overlying pelagic sequence. Nannofossils recovered from the infilling of a large rudist fragment in Core 12 are consistent with the age inferred from planktonic foraminifers. Two rudist fragments were tentatively identified as *Eoradiolites* sp. and *Texicaprina* sp. Both forms are common in the Albian although they are not restricted to this stage. The lower part of this unit (Core 536-16 through 536-21-1, 34 cm) can be dated as late Aptian. Because of the poor recovery (4%), it is impossible to determine if this unit was deposited continuously or intermittently. The rare benthic foraminifers belonging to the carbonate platform community are consistent with the age inferred.

The fourth unit, dolomite, is devoid of diagnostic fossils. According to the sedimentologic interpretation suggesting an advanced diagenetic stage, this dolomitic unit is inferred to be considerably older than the overlying late Aptian–latest Albian carbonate sequence of Unit III.

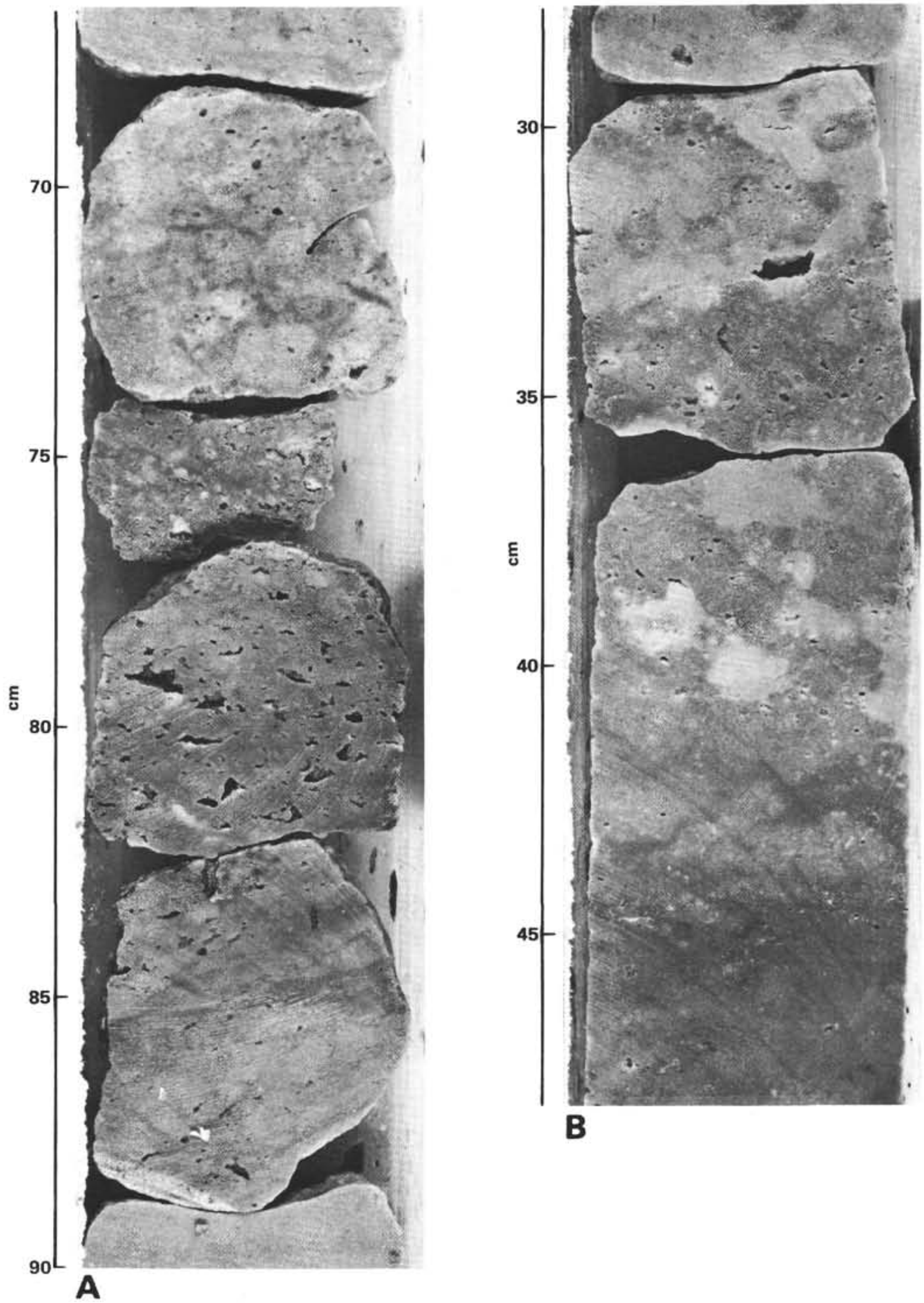

Figure 7. Core photos illustrating various textures of dolomite encountered in Unit IV. A. Homogeneous, massive, fine-grained dolomite with irregular vugs (536-21-1, 67–90 cm). B. Burrow-mottled dolomite (536-21-2, 28–48 cm). C. Laminated or banded dolomite with intraformational clasts and breccias (536-22-2, 95–120 cm). D. Medium-grained "sucrosic" dolomite (536-23-3, 15–40 cm).

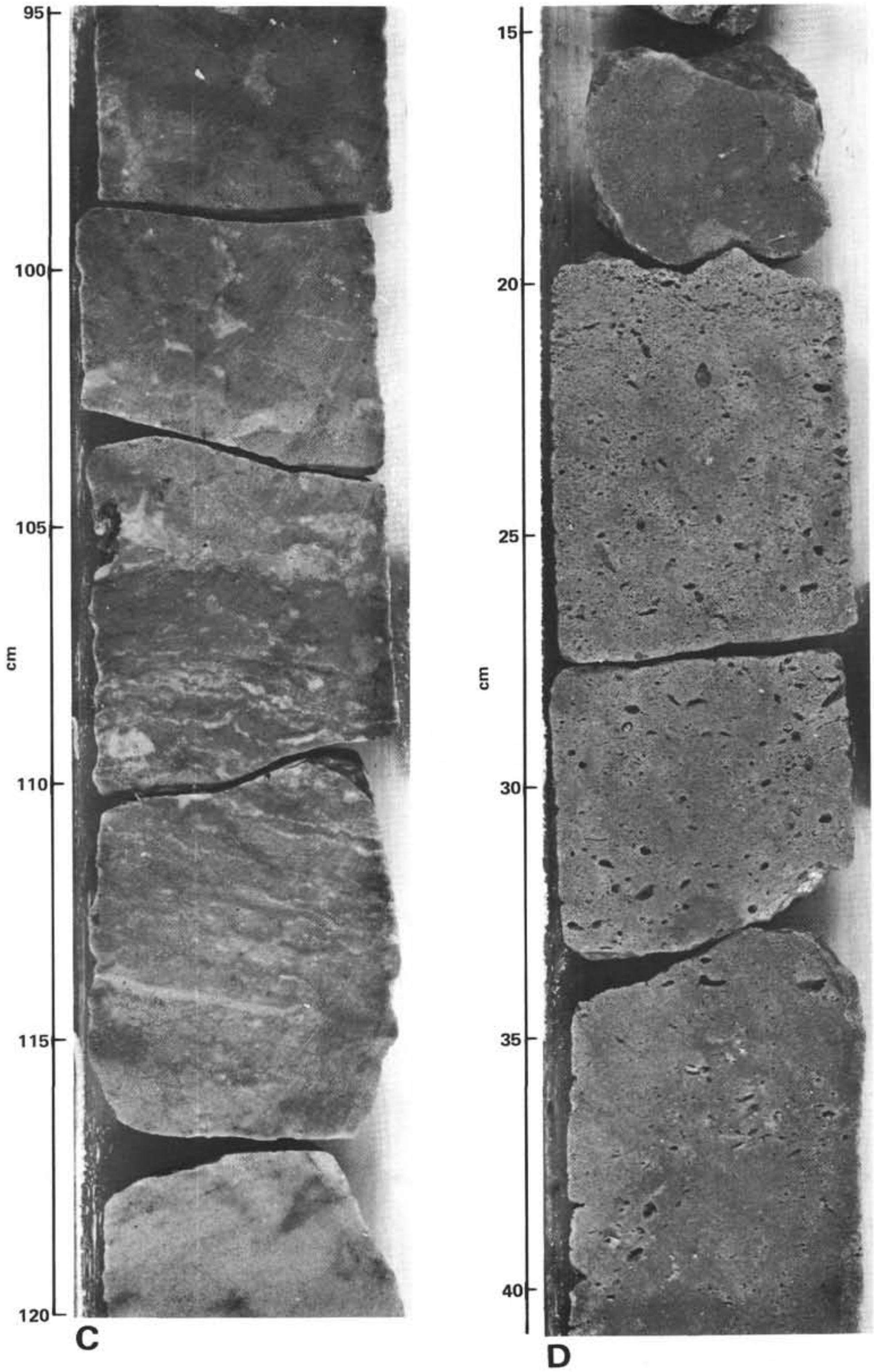

Figure 7. (Continued).

Foraminifers

Foraminiferal content from Site 536 can be divided into three groups, which correspond to major lithologic units. Cores 1 through 9 are composed mainly of foraminiferal-nannofossil ooze and chalk, which yield rich foraminiferal assemblages ranging from Pleistocene down to Maestrichtian. The interval from Core 536-10 to 536-21-1, 34 cm consists of limestone containing shallow-water skeletal debris with infrequent interbeds of micritic limestone with some pelagic microfauna. Planktonic specimens are rare in this interval and could be identified at only a few horizons. The interval from 536-21-1, 35 cm to total depth (Core 23) is composed of dolomite in which no foraminifers were found.

Holocene foraminiferal fauna associated with abundant pteropods is confined to the uppermost 2–3 cm of Core 1, of which the remaining portion through most of Core 2 yielded very rich planktonic foraminiferal faunas of late Pleistocene age. Among the species recognized are *Globorotalia tumida, G. pachytheca, Globigerinoides ruber* (pink), *Pulleniatina finalis, G. conglobatus,* and *Globorotalia inflata.* Pteropods are abundant. Benthic foraminifers are characteristic of lower bathyal environment, consistent with the water depth of 2808.5 m at Site 536.

Samples from 536-2,CC through Core 536-3 yielded a rich planktonic foraminiferal fauna and rare pteropods. The co-occurrence of *G. margaritae* with *Globigerina nepenthes* and *Sphaeroidinella dehiscens* allows correlation of this interval with Zone MPL2 (= middle of *Globorotalia margaritae* Zone) dated as early Pliocene.

Cores 4 and 5 contain late Miocene planktonic faunas, attributable to the medium and lower parts of Zone N16 (= *G. acostaensis/G. merotumida* Zone) respectively. Specifically, few specimens of *Globigerinoides extremus* and *Globorotalia humerosa* occur in Core 4, but they are absent in Core 5.

Core 6, a gray clayey nannofossil ooze, contains a very poor planktonic foraminiferal fauna, in which, however, *G. siakensis* could be identified. This taxon becomes extinct at the end of Zone N14, the penultimate zone of the middle Miocene. The lack of other age-diagnostic forms prevents a precise zonal attibution within the middle Miocene. Glauconite is abundant in the washed residues of this interval. The poor fauna is probably due to heavy dissolution.

Core 7 and the topmost 8 cm of Core 8 yielded very rich planktonic foraminiferal faunas. The concurrence of *G. peripheroacuta, G. peripheroronda, Orbulina universa, G. archaeomenardii,* and forms transitional to *G. praemenardii* allows one to attribute this interval to Zones N11/N10, dated as middle Miocene.

At 536-8-1, 10 cm, there is a sharp change from bluish gray, Neogene ooze to yellowish gray, upper Oligocene ooze-chalk (Zone P22 = *Globigerina angulisuturalis* Zone). The remainder of Core 8 is composed of the same lithic and faunal unit.

Interval 536-9-1, 1–3 cm consists of well-indurated, white, lower Eocene chalk of the *Acarinina pentacamerata* Zone (= Zone P9), as inferred from thin-section examination. Below that are approximately 11 cm of upper Paleocene of the *Planorotalites pseudomenardii* Zone, again based on thin-section identification. Most of the remainder of Core 9 (536-9-1, 15 cm to 536-9-5, 69 cm) is composed of yellowish brown, Paleocene chalk with rich foraminiferal faunas of the following zones:

9-1, 15 cm to 9-3, 17 cm	*Planorotalites pseudomenardii* Zone	upper Paleocene
9-3, 18 cm to 9-4, 80 cm	*"Morozovella" trinidadensis* Zone	lower Paleocene
9-4, 81 cm to 9-5, ~40 cm	*Subbotina pseudobulloides* Zone	lower Paleocene
9-5, ~41 cm to 9-5, 69 cm	*"Globigerina" eugubina* Zone	lower Paleocene

The Cretaceous/Tertiary boundary occurs at 536-9-5, 70 cm. However, the earliest Tertiary *"G." eugubina* zonal fauna infills burrows for at least 10 cm below the boundary.

Lithification and composition vary, and dissolution of microfossils increases below the boundary. Specimens recovered from the core catcher of Core 9 are highly dissolved and fragile. Recognizable species include: *Pseudotextularia elegans, Racemiguembelina fructicosa* (rare), *Globotruncana fornicata, G. arca, G. linneiana* group, *G. stuartiformis, G. stuarti, G. tricarinata, G. contusa, G. ventricosa, Pseudoguembelina excolata,* and *Ventilabrella manuelensis.* The assemblage suggests upper Maestrichtian, although several critical forms of the *Abathomphalus mayaroensis* Zone were not seen.

The interval from Core 536-10 through 536-21-1, 34 cm is characterized by two different lithofacies: limestone containing shallow-water skeletal debris and pelagic micritic limestone. These two lithotypes occur in differing proportions throughout the mentioned interval: from Core 10 to 536-16-1, 38–44 cm, coarser limestones were primarily recovered, but pelagic limestones are rare; from 536-16-1, 45 cm to 536-21-1, 34 cm, pelagic limestones are predominant, and the limestone with shallow-water debris becomes a minor lithologic component, frequently represented only by thin layers within the pelagic limestones. The recovery is too poor to establish if the mentioned trend is real or is a drilling artifact.

In addition to abundant recrystallized radiolarians, the pelagic limestones contain some planktonic foraminifers that could be reliably identified in thin section. The richest assemblages occur in samples at:

536-11-1, 13–15 cm, which yielded *Planomalina buxtorfi* (rare) and *Rotalipora appenninica R. ticinensis.* This assemblage characterizes the lower part of the *P. buxtorfi* Zone, the youngest biozone of the Albian (= Vraconian).

536-16-1, 0–10 cm, which yielded *Hedbergella gorbachikae, H. trochoidea,* and forms attributable to primitive *P. cheniourensis.* This assemblage can be assigned to the *H. gorbachikae* Zone, dated as late Aptian.

536-19-1, 3–5 cm, which yielded a poor planktonic foraminiferal assemblage also attributable to late Aptian *H. gorbachikae* Zone.

536-20-1, 5–7 cm, which yielded an assemblage similar to that in 536-16-1, 0–10 cm, except for *H. gorbachikae*. This assemblage, in the absence of the latter taxon, was attributed to the *Globigerinelloides algerianus* Zone, also belonging to the late Aptian.

536-21-1, 32–34 cm, the last limestone within the dolomitic unit, which contains a relatively rich planktonic foraminiferal assemblage of the *G. algerianus* Zone, late Aptian in age.

Abundant radiolarians, most of them recrystallized, occur with planktonic foraminifers in the lower part of the unit. In the upper part, they are absent or occur rarely from Cores 10 through 14. Only one layer, belonging to the upper part, in 536-15-1, 31–34 cm, yielded an almost exclusively radiolarian fauna.

A bloom of calcispherulids was recorded in 536-17-1, 5–6 cm.

Limestones are mainly composed of shallow-water debris that vary in size throughout the whole interval: larger debris in the upper part (Core 536-10 to 536-16-1, 38–44 cm), minute in the lower part (536-16-1, 45 cm to 536-21-1, 35 cm).

In the upper part, large fragments of rudists, echinoids, and shells of large pelecypods are the main skeletal components. Foraminifers are rare with a single specimen of *Trocholina* sp. and a few small valvulinids recorded in each sample. One specimen of a possible *Paracoskinolina* occurs in 536-16-1, 38–44 cm. Calcareous algae are also rare; a few fragments attributable to Solenoporaceae (*Parachaetetes*?) (red algae), to Dasycladaceae (*Cymopolia*?) and Codiaceae (*Cayeuxia*?) (both green algae) occur in a few samples from Cores 10, 13, and 14.

In the lower part, clasts and fragments are mostly too small to be diagnostic except for echinoid debris, which are always a common component of the coarser layers. Ghosts of possible corals occur in 536-20-1, 4–5 cm and 536-21-1, 5–10 cm. *Acicularia* sp. (small dasycladacean) and possibly *Cayeuxia* (codiacean) occur in 536-20-1, 7–8 cm. Among the shallow-water benthic foraminifers, the only significant occurrences are a single specimen of an agglutinated *Paleocoskinolina*? in 536-20-1, 7–8 cm and several specimens of *Trocholina* sp. in 536-20-1, 10–11 cm.

The dolomite unit (536-21-1, 35 cm through Core 536-23) is barren except for some ghosts of possible incrusting algae, which occur in some samples of Core 23.

Calcareous Nannofossils

Only the Tertiary to Maestrichtian biogenic carbonate sequence at Site 536 contains age-diagnostic nannofossil assemblages. The Lower Cretaceous limestone sequence is largely barren of nannofossils. One sample (536-12-1, 0–1 cm) did, however, contain some recognizable nannofossil material. The sediment filling a void in a rudist grainstone yielded a poorly preserved, very sparse nannofossil assemblage with *Retacapsa angustiforata, Prediscosphaera cretacea*, and *Watznaueria barnesae*. This indicates that the void-filling material is of Albian to Maestrichtian age. The dolomite sequence is devoid of nannofossils.

The Tertiary to Maestrichtian pelagic carbonate sequence contains sediments of all Tertiary epochs, although the biostratigraphic sequence is by no means continuous. Much of the Tertiary is represented by unconformities with hiatuses of varying length.

Cores 536-1 to Section 536-2-2 contain nannofossil ooze with well-preserved assemblages including *Emiliania huxleyi, Gephyrocapsa oceanica, G. caribbeanica*, and *Ceratolithus cristatus*. This interval is assigned to the *E. huxleyi* Zone (CN15) of the late Pleistocene to Holocene.

The interval from 536-2-2, 140 cm through Core 536-3 contains nannofossil ooze of the *Amaurolithus tricorniculatus* Zone (CN10) of early Pliocene age. Samples within this interval contain assemblages that include *C. acutus* (sporadic), *Discoaster brouweri, D. pentaradiatus, D. surculus*, and *Sphenolithus neoabies*. Nannofossils are abundant and well preserved.

Three nannofossil biozones are represented in the nannofossil oozes of Cores 4 to 8 (partim). Cores 4 through 5 contain *D. quinqueramus, D. berggrenii*, and *D. surculus*, indicating the *D. quinqueramus* Zone (CN9). Cores 4 through 5 also contain a large component of a reworked, lower Miocene nannofossil assemblage that includes *D. hamatus, D. bollii*, and *D. neohamatus*. Core 6 contains *Reticulofenestra pseudoumbilica, D. bollii, D. exilis, D. braarudii*, and sporadically occurring *D. kugleri*. Core 6 has been assigned to the *D. exilis* Zone (CN5) of middle Miocene age. The interval from Core 536-7 through 536-8-1, 0–1 cm contains assemblages that include *S. heteromorphus, R. pseudoumbilica, Cyclicargolithus floridanus, D. variabilis*, and *Cyclococcolithina macintyrei* (rare). This interval is assigned to the *S. heteromorphus* Zone (CN4) of (late) early Miocene to (early) middle Miocene age. The Miocene interval is separated from the underlying Oligocene by a sharp, curved (concave downwards) lithologic boundary.

The interval from 536-8-1, 7–9 cm through 536-8,CC is assigned to the *S. ciperoensis* Zone (CP19) of late Oligocene age. The assemblage recovered from samples of this nannofossil chalk includes *S. ciperoensis, D. deflandrei, Cyclicargolithus floridanus, Cyclicargolithus abisectus*, and *Dictyococcites bisectus*. Preservation of nannofossils within this interval is moderately good to excellent.

The part of the Eocene datable by nannofossils is represented by 1 cm (536-9-1, 0–1 cm) of hard nannofossil chalk. A moderately preserved assemblage containing *Discoaster lodoensis, D. sublodoensis, D. barbadiensis*, and *S. radians* indicates that this chalk is in the *D. sublodoensis* Zone (CP12) of (late) early Eocene to (early) middle Eocene age. This chalk also contains reworked Paleocene species including *D. multiradiatus, Toweius eminens*, and *Fasciculithus tympaniformis*. This Eocene chalk overlies a 2–3 cm thick chert bed of indeterminant age.

Samples from the interval from 536-9-1, 19–20 cm through 536-9-3, 19–20 cm contain nannofossil assemblages that include *D. multiradiatus, D. mohleri, T. eminens, Chiasmolithus californicus*, and *F. tympani-*

formis. This interval is assigned to the *D. multiradiatus* Zone (CP8) of late Paleocene age.

The recovered interval from 563-9-3, 111-113 cm to 563-9,CC contains a record of relatively continuous pelagic sedimentation across the Tertiary/Cretaceous boundary. The interval from 563-9-3, 111-113 cm through 563-9-4 contains an assemblage that includes *Cruciplacolithus tenuis, Markalius astroporus, Zygodiscus sigmoides*, and *Chiasmolithus danicus*. This interval is assigned to the *C. danicus* Zone (CP2) of early Paleocene (Danian) age. The interval from 563-9-5, 0-1 to 563-9-5, 59-60 cm is assigned to the *Z. sigmoides* Zone (CP1) of earliest Paleocene (Danian) age. The interval in CP1, and to some extent CP2, contains abundant thoracosphaerids and braarudisphaerids. The interval from 563-9-5, 95-96 cm to 563-9,CC contains a late Maestrichtian assemblage including *Micula mura, Lithraphidites quadratus*, and other Cretaceous species. This interval is assigned to the *M. mura* Zone of late Maestrichtian age.

GEOCHEMISTRY

There were no rocks encountered at Site 536 that had organic matter, therefore, no samples were collected for analysis. There were no shows of hydrocarbons.

Eighteen carbonate bomb samples were run for percent $CaCO_3$; the results are tabulated in Table 3. Two interstitial water samples were run for chemistry; those results are given in Table 4.

PALEOMAGNETISM

At Site 536, deposition was relatively continuous across the Cretaceous/Tertiary boundary, according to the paleontologic and lithologic observations. During the past few years, the precise definition of the Cretaceous/Tertiary boundary has been the subject of intensive research. Magnetostratigraphy is particularly important in this context because it enables us to correlate between geologic sequences that have no common fauna. The Cretaceous/Tertiary boundary has been studied paleomagnetically at several localities: a pelagic carbonate sequence in Gubbio, Italy (Roggenthen and Napoleone, 1977); terrestrial sequences in the San Juan Basin, New Mexico (Butler et al., 1977) and Red Deer Valley, Alberta (Lerbekmo et al., 1979); and at various DSDP sites[3]. The agreement between these studies is indeed remarkable, but minor discrepancies do exist. At Site 536, paleomagnetic sampling was confined to a well-dated, continuous sequence of Danian and Maestrichtian ooze, chalk, and limestone immediately above and below the boundary (536-9-3 to 536-9-6). The purpose of this sampling is to compare paleomagnetic data across this boundary with data from the other studies mentioned above.

A total of 32 oriented samples were collected at approximately 15-cm spacing in between Sections 536-9-3 and 536-9-6. Because of the soft nature of the sediment, all but two samples were collected in plastic boxes. Before the sampling was started, the boxes had been measured and found to be below the noise level of the onboard Digico magnetometer (approximately 2×10^{-7} emu). As an additional safeguard, however, the boxes were demagnetized in three perpendicular directions at 600 Oe before being used for sampling. Some drilling disturbance was observed; to obtain the best results, we took samples from the center of the core and avoided sampling at depths where color banding, suggestive of bedding, was not horizontal.

The natural remanent magnetization (NRM) of the samples was measured over a period of a few days. Repeat measurements approximately 2 days later showed a dramatic change in the direction as well as a decrease in intensity of magnetization of many samples. This observation indicates that the samples can readily acquire a viscous magnetization. Because of this and because many samples had intensities close to the noise level of the shipboard magnetometer, no further measurements were carried out during the cruise.

In the paleomagnetic laboratory of The University of Texas, Galveston Marine Geophysics Laboratory, the samples remained in a magnetically shielded room (ap-

Table 3. Carbonate contents of selected samples, Hole 536.

Core-Section (interval in cm)	$CaCO_3$ (%)
1-1, 142-143	39
1-2, 40-42	64
1-2, 60-62	70
1-3, 48-49	44
1-3, 60-62	53
2-2, 4-5	69
3-3, 80-81	71
4-4, 77-78	75
5-2, 76-77	75
6-1, 86-87	35
6-1, 123-124	19
6-1, 140-141	45
7-2, 9-10	57
7-2, 118-119	77
8-1, 4-5	73
8-1, 13-14	82
8-4, 70-71	83
9-4, 81-82	86

Table 4. Interstitial water analyses, Site 536.

	Surface seawater	IAPSO standard	Sample 536-3-1, 144-150 cm	Sample 536-8-1, 140-150 cm
Sub-bottom depth (m)			19.4-19.5	66.9-67.0
pH	5.86		6.72	7.33
Alkalinity (meq/l)	2.468		3.578	2.956
Salinity (‰)	37.3	36.1	36.9	37.3
Calcium (mmol/l)	10.61		10.26	11.48
Magnesium (mmol/l)	54.36		51.93	52.54
Chlorinity (‰)	19.90		19.62	19.65

[3] For example, Site 384 (Tucholke, Vogt, et al., 1979), Site 524 (Hsü, LaBrecque, et al., in press), and Site 527 (Moore, Rabinowitz, et al., in press).

proximately 100 gamma residual field) throughout the experimental procedures to avoid any effects of viscous magnetization. The samples were measured with a cryogenic magnetometer and demagnetized in peak alternating fields 25, 50, 75, 100, 150, 200, 300, and 400 Oe. Most samples responded to demagnetization in a very similar manner, suggesting a very homogeneous lithology. Three distinct components of magnetization can be recognized in most samples. Component 1 is removed by demagnetization to 25 Oe and is probably the result of magnetic contamination. Component 2 is usually erased between 25 and 100 Oe, and Component 3 decays toward the origin at higher fields (100–400 Oe). With one exception, Component 2 is of normal polarity with inclinations averaging 45°. Component 3, on the other hand, has a negative inclination for all but two samples with a mean of −45.6°.

The most straightforward interpretation is that Component 2 is a present-field overprint and that Component 3, with its higher coercive force, is the primary magnetization. However, this is not necessarily correct. Because the magnetic inclination of this site (41°) has changed only by 0.2° since the Paleocene, Component 2 could have been acquired during any normal epoch since deposition. Component 3, although more stable, could have been acquired secondarily as a result of chemical changes during a reverse epoch. Therefore, it is possible that either component is the primary component or that neither is.

Both components exhibit reversal patterns that are incompatible with expected reversal sequence (e.g., LaBrecque et al., 1977) (Fig. 8). The only possible correlation, between Component 3 and expected sequence, would require a variable and extremely fortuitous sedimentation rate that increased during reverse epochs. If we assume that the results of other magnetic studies of the Cretaceous/Tertiary boundary are valid, the only other explanation of the discrepancy is that the samples were remagnetized twice after deposition, once during a normal epoch and once during a reverse one. It should be emphasized that the measurements are of excellent quality and that the lack of correlation cannot be attributed to unreliable measurements.

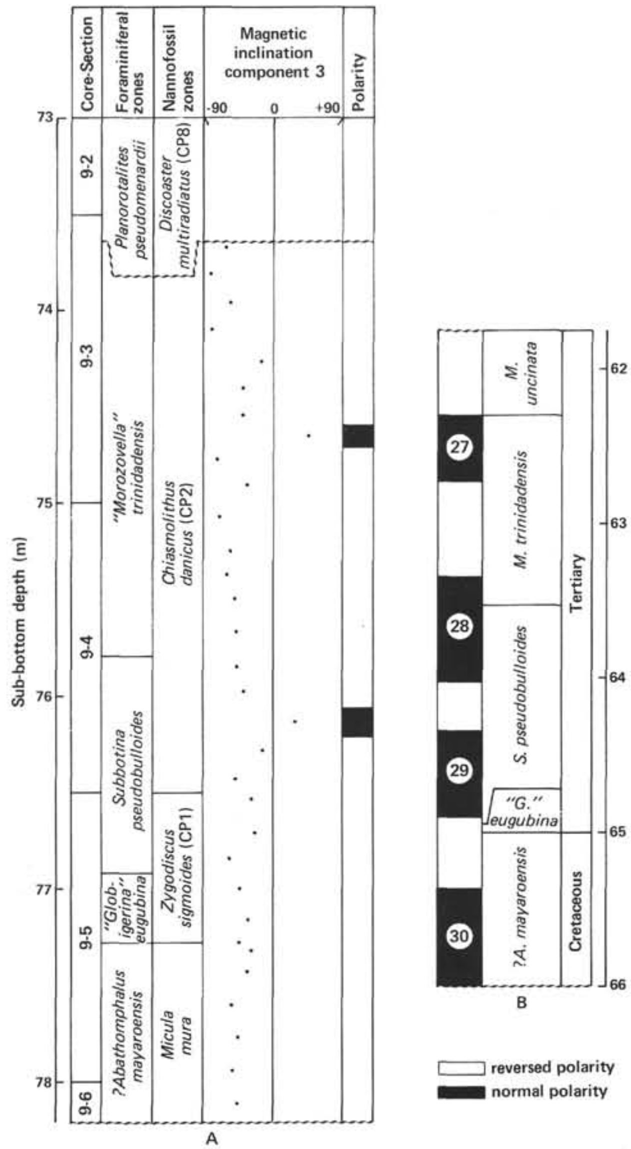

Figure 8. A. Paleomagnetic summary of part of Core 536-9. See text for discussion. B. Gubbio stratigraphy shown for comparison (Gubbio biostratigraphy time scale from LaBrecque et al., 1977).

PHYSICAL PROPERTIES

Sonic velocity was measured by the Hamilton Frame method; 2-minute GRAPE measurements for obtaining density and porosity data, as well as thermal conductivity measurements by the Needle Probe method, were taken for individual samples taken from the cores. Continuous GRAPE measurements were taken for all the cores immediately after the recovery. Mudline temperature and bottom-hole temperature at sub-bottom depths of 51.5 and 80 m were obtained by means of the Heat Flow Probe operated by DSDP staff. The heat flow value of the area was calculated and compared with other local data. Results of individual measurement are listed in Table 5 and displayed graphically in Figure 9. They are discussed separately below.

Sonic velocity distribution with respect to sub-bottom depth is characterized by several groups, each with considerably different velocity values. Between each group there are thick sections from which samples large enough to allow physical measurements were not obtained. Although the exact boundary among these three groups in terms of the sonic velocity could not be clarified, the entire section of 0–213 m could be subdivided into the following four units (also see Figs. 2 and 9):

Sonic unit	Sub-bottom depth (m)	Comment
A	0–69	Marked by velocities close to that of the seawater
B	70–81	Related to a sharp increase in velocities
	82–107	No samples for physical measurements
C	108–149	Marked by intermediate velocities
	150–184	No samples for physical measurements
D	185–206	Characterized by high velocities and impedances

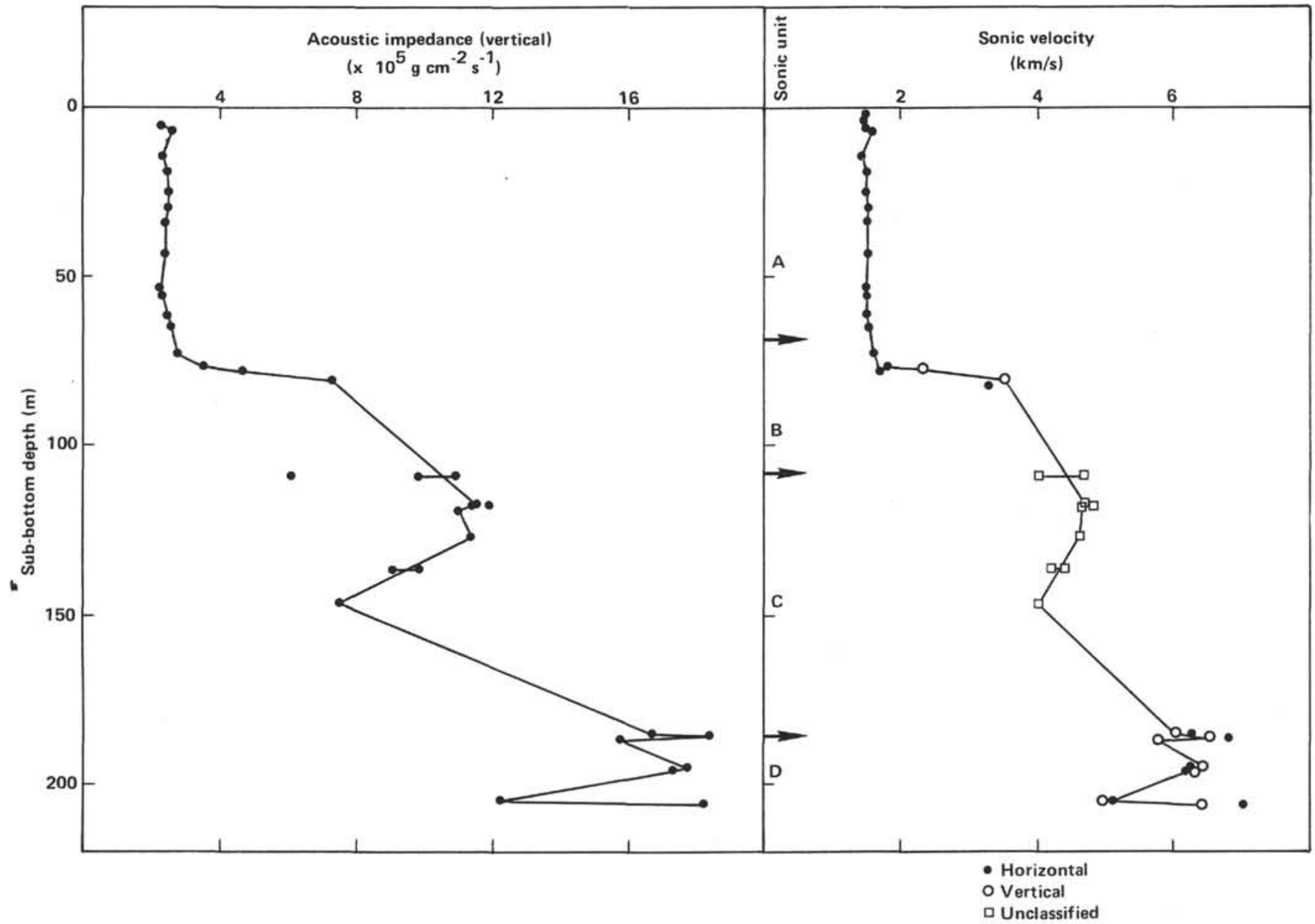

Figure 9. Profiles of selected physical properties, Site 536.

Statistical treatments attempted on the samples according to this subdivision are listed in Table 6. It is noted, however, that for Unit A the velocity values are nearly constant. In Unit C, the cores were highly fragmented and the velocity values only reflect those of arbitrary orientations with respect to the geologic formations (Table 5).

Velocity, density, and porosity data are correlated graphically in Figure 10. There is a clear linear relation between the density and porosity for both dolomites and limestones. Dolomites, which were observed mostly in Sonic Unit D (Lithologic Unit IV), are aligned along a line markedly different from the limestone group.

Heat flow measurements were run twice at sub-bottom depths 51.5 and 80 m. The probe was set at a 1-minute sampling rate and then lowered by the sand line into the hole. Lowering was stopped at 12 m above the bottom of the hole for about 15 minutes before stabbing into the bottom sediment in order to equilibrate to the surrounding temperature. The probe was kept in the sediments at the bottom of the hole for 20 minutes before retrieval. Mudline temperature was measured on the second run by stopping the probe at the mudline for 20 minutes while on the way out of the hole. The changes of temperature with time are shown in Figure 11. Three temperature measurements (i.e., mudline, 51.5 and 80 m sub-bottom depth) are plotted in Figure 12. The temperature probe operation for depths greater than 80 m sub-bottom was not attempted because the sediment layer became too firm to enable us to send the probe down without fear of its destruction. Resultant temperature gradient in this hole is derived as 13.75°C/km (Fig. 12).

The thermal conductivity of the sediments between 0 and 80 m sub-bottom depth was measured on eight samples. The values are averaged by simple arithmetic to give 2.77×10^{-3} (cal deg^{-1} s^{-1} cm^{-1}) (Fig. 12). The heat flow value was determined as 0.38 heat flow units (HFU) (μcal cm^{-2} s^{-2}). This is somewhat lower than the average local HF (0.83 HFU) determined from four nearby values (Martin and Case, 1975). The reason for this difference is not clear.

SEISMIC STRATIGRAPHY

Site 536 is located along seismic Line GT3-75 in an area where an inferred basement block is overlain by only a relatively thin (200–300 m) sediment cover (Fig. 3). A close-up view of the seismic line at the site is shown in Figure 13. The strong reflector or acoustic basement at about 3.95 s was inferred to be the top of a basement block. This was the main objective of the hole.

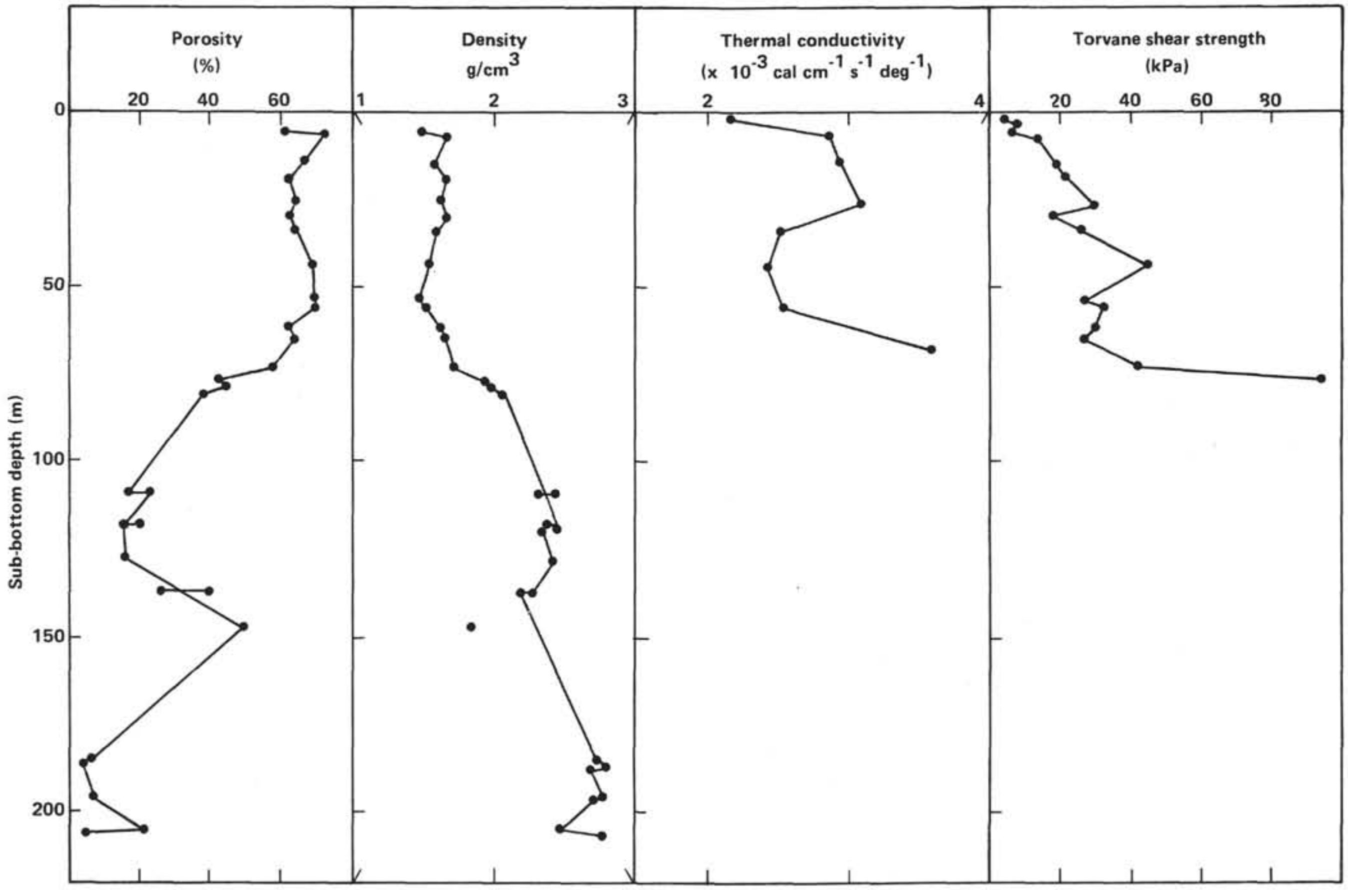

Figure 9. (Continued).

Another strong reflector seen on the seismic line at about 3.8 s was interpreted as a major unconformity separating a thin section of mainly Tertiary oozes and chalks (inferred from previous drilling at Sites 96 and 97; Worzel, Byrant, et al., 1973) from older Meosozoic rocks below. This prominent unconformity can be traced to the south and west where it splits into two major unconformities (e.g., southern end of Line GT3-75, Fig. 13). The upper of the two unconformities has been correlated with a prominent Gulf-wide reflector/unconformity tentatively dated as mid-Cretaceous (Buffler et al., 1980, 1981) and designated MCU on the seismic sections. The lower unconformity forms the top of a thick seismic sequence that covers the entire western part of the southeastern deep Gulf south of the drill site. This sequence has been interpreted as a broad, early Mesozoic, shallow-water platform (see Fig. 2, schematic cross section, in Introduction and Explanatory Notes chapter). These rocks appear to correlate with rocks lying well below the oldest rocks drilled at Site 535 (Berriasian) (site chapter, Site 535, this volume). This makes the platform sequence probably Jurassic or older. A thin part of this sequence may extend to the drill site area and may correspond to the dolomite unit at the base of the hole. (Fig. 13).

This sequence thins and onlaps to the northwest against still another prominent unconformity (Fig. 13). This older unconformity truncates an older tilted sequence, inferred to be equivalent to the Triassic–Early Jurassic rift basins that occur all along the east coast of the United States and along the northern Gulf coast and in Mexico. The reflector at the base of the rift sequence appears to merge updip with the acoustic basement at the drill site, supporting the contention that the reflector represents true basement.

Drilling at Site 536 encountered about 80 m of Late Cretaceous through late Tertiary ooze and chalk overlying approximately 110 m of mid-Cretaceous (Aptian-Albian) skeletal limestone interpreted to be a talus apron. The remainder of the hole to 213 m consisted of dense dolomite of shallow-water origin but of unknown age. There was a sharp increase in sonic velocity from 1.6 to 3.1 km/s in the lower part of the ooze-chalk section at about 70 m depth (Fig. 9). There probably is another increase in sonic velocity at the contact between the chalks and the underlying skeletal limestones, as the sonic velocities in the limestones measured farther down in the hole average about 4.5 km/s (Fig. 9). Taken together, these changes represent a large increase in acoustic impedance and should produce a strong reflector. The prominent reflector/unconformity at about 3.85 s at the drill site, therefore, is correlated with this overall change in lithology. Because of the resolution of the seismic tool, this reflector represents a condensed sequence ranging

Table 5. Physical properties for Site 536.

Core-Section (interval in cm)	Depth (m)	Sonic velocity (km/s) H ∥	V ⊥	2-minute GRAPE Wet-bulk density (g/cm³) H	V	2-minute GRAPE ϕ (%)	Gravimetrics Wet-bulk density (g/cm³)	Gravimetrics ϕ (%)	Gravimetrics Water content (%)	Acoustic impedance (V) ($\times 10^5$ g cm^{-2} s^{-1})	Torvane shear (kPa)	Thermal conductivity ($\times 10^{-3}$ cal deg^{-1} cm^{-1} s^{-1})	Lithology
1-2, 60-62	2	1.529									4.31	2.16	
1-3, 60-62	4	1.524									8.13		
2-2, 20-22	6	1.526					1.50	72	48	2.289	7.66		
2-2, 120-122	7	1.574					1.68	61	36	2.644	14.3	2.86	
3-1, 104-106	15	1.488					1.59	66	42	2.366	18.7	2.94	
3-4, 85-87	19	1.503					1.66	62	38	2.450	22.0		
4-3, 105-107	27	1.538					1.63	64	39	2.507	30.6	3.07	
4-5, 105-107	30	1.541					1.65	63	38	2.543	18.2		Carbonate ooze
5-2, 141-143	34	1.531					1.60	64	40	2.450	26.7	2.54	
6-2, 39-41	44	1.568					1.53	69	45	2.399	45.1	2.45	
7-2, 138-140	54	1.534					1.50	69	46	2.301	27.7		
7-3, 125-135												2.54	
7-4, 57-59	56	1.538					1.53	69	45	2.353	31.6		
8-1, 131-132	62	1.541					1.62	63	39	2.496	29.67		
8-3, 128-130	65	1.575					1.64	63	38	2.583	26.81		
8-5, 80-85												3.59	
9-2, 85-88	73	1.637					1.71	58	34	2.799	42.13		
9-5, 89-90	77	1.800		2.02		40.6	1.97	43	22	3.546	95.8		Chalk
9-6, 12-14	78	1.760	2.342	1.89		48.4	2.00	44	22	4.684	—		
10-1, 55-58	81	3.350	3.583	1.98		43.0	2.05	38	18	7.345	—		
13-1, 13-15	109	4.071		2.08		37.0	2.41	17	7	9.811			
13-1, 74-76	109	4.714		2.33		22.1				10.984			
14-1, 4-6	118	4.771		2.38		19.1				11.355			
14-1, 37-39	118	4.858		2.52		10.7	2.45	15	6	11.902			Limestone
14-1, 84-86	119	4.023		2.36		20.3				10.910			
15-1, 4-6	128	4.664		2.93		16.1				11.334			
16-1, 18-20	137	4.470		2.02		40.6	2.22	27	12	9.029			
16-1, 43-45	137	4.299		2.26		26.3				9.716			
17-1, 18-20	147	4.074		1.85		50.7				7.537			
21-1, 27-30	185	6.381	6.051	2.81		<0	2.75	6	2	16.640			
21-1, 129-131	186	6.856	6.536	2.79		<0	2.80	4	1	18.301			
21-2, 77-80	187	5.686	5.762	2.71		<0				15.615			
22-1, 117-119	195	6.280	6.472	2.81	2.74	<0				17.733			Dolomite
22-2, 53-56	196	6.227	6.339	2.76	2.76	<0	2.74	6	2	17.369			
23-2, 44-47	205	5.163	5.109	2.53		10.1	2.49	20	8	12.721			
23-2, 73-77	206	7.080	6.496	2.74		<0	2.79	4	2	18.124			

Note: ϕ = porosity; H = horizontal; V = vertical.

Table 6. Groupings of physical properties, Site 536.

Sonic unit	Sub-bottom depth (m)	Density (g/cm³)	Porosity (%)	Sonic velocity (km/s) V	H	Acoustic impedance (V) ($\times 10^5$ g cm^{-2} s^{-1})	Thermal conductivity ($\times 10^{-3}$ cal deg^{-1} s^{-1} cm^{-1})	Lithology[a]
A	0-69	1.59	65	1.61		2.5	2.77	Ooze
B	70-81	1.93	45	3.11	2.25	4.8		Chalk/limestone
C	108-149	2.27	25	4.53		10.3		Limestone
D	185-206	2.73	8	6.11	6.24	16.6		Dolomite

Note: V = vertical; H = horizontal.
[a] Lithologic units are divided as follows: I, 0-61 m; II, 61-80 m; III, 80-188.5 m; IV, 188.5-213 m sub-bottom depth.

from late Albian to Eocene. The major hiatus represented by the unconformity, however, covers most of the Late Cretaceous.

The ooze and chalk section drilled probably correlates with the relatively transparent unit seen on the seismic section lying above the unconformity. Converting this time section (0.12 s) to depth using a velocity 1.6 km/s gives approximately 96 m of section, fairly close to the 70 m drilled. The actual drill site is slightly upslope from the seismic line and perhaps the section is slightly thinner here.

Next, it should be decided whether or not the dolomite corresponds to the inferred basement reflector, because this change in lithology represents another large impedance change and should produce a strong reflector. The approximate 2-way time between the two strong reflectors is about 0.13 s. Using the average interval velocity determined for the skeletal limestone (4.53 km/s), the thickness of the seismic unit is 294 m, much thicker than the 110 m for the limestone drilled. It is concluded, therefore, that the acoustic basement was not reached.

A close look at the seismic section indicates that the reflector forming the prominent unconformity is about 0.05-s thick (2-way) at the site location and appears to consist of several major unconformities merged together as discussed above (Fig. 13). The 2-way time interval

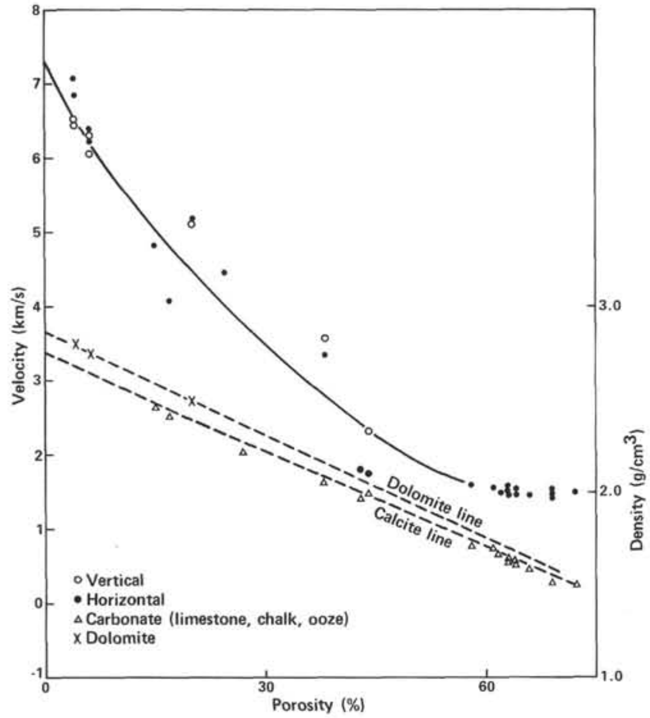

Figure 10. Relationships between density and porosity and between velocity and porosity for Site 536. Density data for dolomites are separated from other carbonates at this site to illustrate trends.

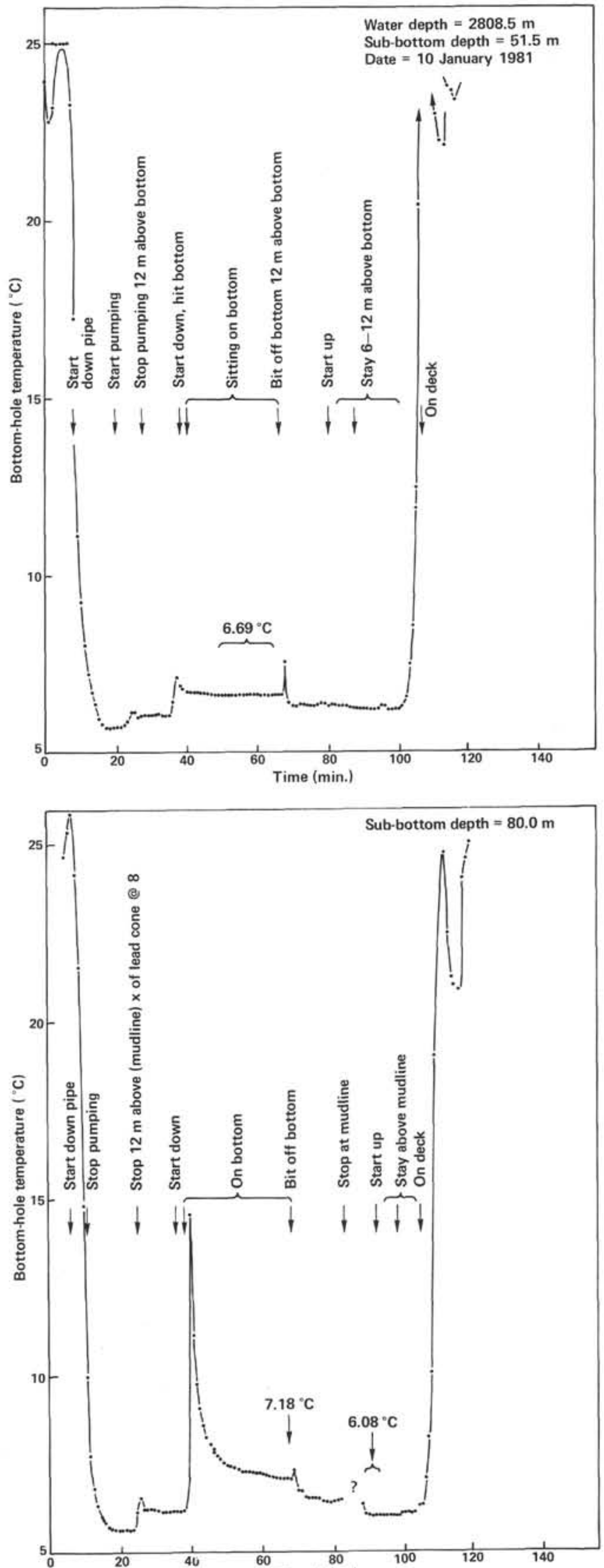

Figure 11. Heat flow probe temperature measurements at Site 536 (i.e., mud line, 51.5 and 80 m sub-bottom depths).

represented by the 110-m section of limestones is also only about 0.05 s, which is near the resolution of the seismic tool. Thus, the top of the dolomite may be masked by the first strong reflector, and it actually may correlate with the lower unconformity where the two separate further to the south. One interpretation for the big unconformity drilled between the limestones and the dolomites is that it correlates with the seismic unconformity at the top of the inferred early Mesozoic platform sequence discussed above. The dolomites, therefore, could represent rocks deposited as part of this older inferred shallow-water sequence.

Further interpretation of the drilling results using seismic data can be made by looking at a nearby seismic line (SF-3, SF-4), which crosses line GT3-75 just southeast of the drill site (Figs. 1 and 14). This line shows some of the relationships along the Campeche Escarpment. The reflectorless zone at the escarpment is interpreted to represent a mid-Cretaceous (mainly Aptian-Albian) carbonate bank margin with up to 1500 m of relief, whereas the flat-lying reflections behind probably represent platform interior sediments. This interpretation is supported by the Aptian-Albian reef material dredged along this escarpment (Bryant et al., 1969) and drilled at Site 536.

There is a thick wedge-shaped seismic unit at the base of the escarpment, which thickens toward the escarpment (Fig. 14). It appears to fill a broad trough at the base of the escarpment and onlaps up onto the adjacent block. This unit is tentatively correlated with talus apron dredged and drilled. It lies between the two prominent unconformities, which diverge toward the escarpment.

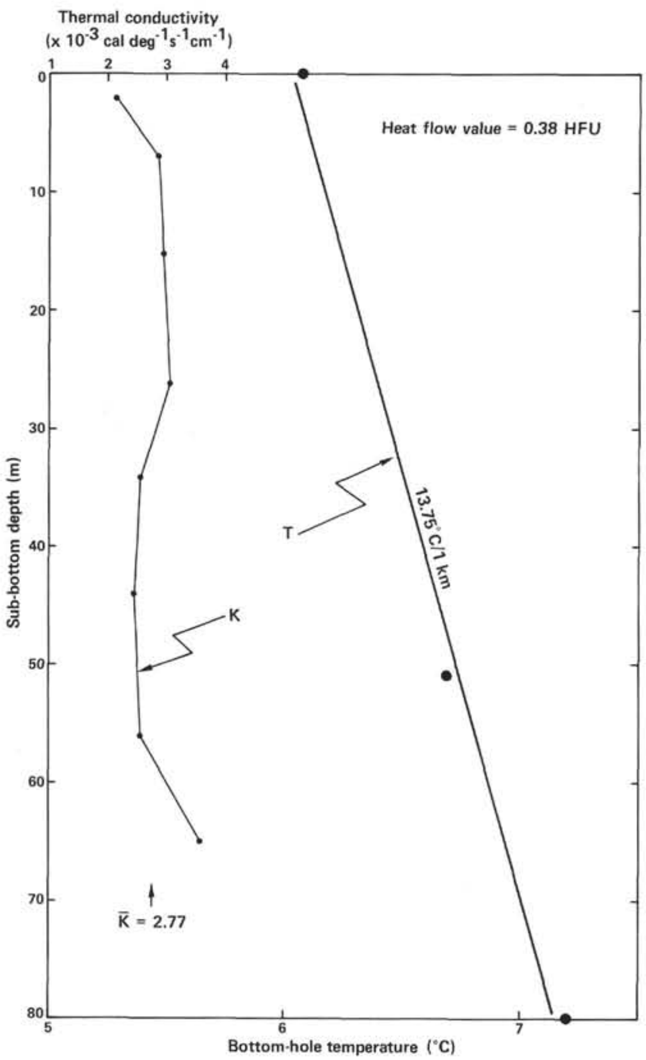

Figure 12. Thermal conductivities (K), bottom-hole temperatures, thermal gradients, and heat flow at Site 536.

The upper unconformity correlates with the MCU, whereas the lower unconformity correlates with the top of the inferred early Mesozoic platform. Again, the dolomites might represent the upper part of the older shallow-water platform.

CONCLUSIONS

The conclusions concerning this site are given in the Summary section earlier in this chapter.

REFERENCES

Bryant, W. R., Meyerhoff, A. A., Brown, N. K., Jr., Furrer, M. A., Pyle, T. E., and Antoine, J. W., 1969. Escarpments, reef trends, and diapiric structures, eastern Gulf of Mexico. *Am. Assoc. Pet. Geol. Bull.*, 53(12):2506–2542.

Buffler, R. T., Shaub, F. J., Huerta, R., Ibrahim, A. B. K., and Watkins, J. S., 1981. A model for the early evolution of the Gulf of Mexico basin. *Oceanol. Acta*, 26th Int. Geol. Congr., Geol. Continental Margins Symp., pp. 129–136.

Buffler, R. T., Watkins, J. S., Shaub, F. J., and Worzel, J. L., 1980. Structure and early geologic history of the deep central Gulf of Mexico basin. *In* Pilger, R. H. (Ed.), *The Origin of the Gulf of Mexico and the Early Opening of the Central North Atlantic Ocean:* Baton Rouge, Louisiana (Louisiana State University), pp. 3–16.

Butler, R. F., Lindsay, E. H., Jacobs, L. L., and Johnson, N. M., 1977. Magnetostratigraphy of the Cretaceous/Tertiary boundary in the San Juan Basin, New Mexico. *Nature*, 267:318–323.

Hsü, K. J., LaBrecque, J. L., et al., in press. *Init. Repts. DSDP*, 73: Washington (U.S. Govt. Printing Office).

LaBrecque, J. L., Kent, D. V. and Cande, S. C., 1977. Revised magnetic polarity time scale for Late Cretaceous and Cenozoic time. *Geology*, 5:330–335.

Lerbekmo, J. F., Evans, N. E., and Baadsgaard, H., 1979. Magnetostratigraphy, biostratigraphy and geochronology of Cretaceous/Tertiary boundary sediment, Red Deep Alley. *Nature*, 279:26–30.

Martin, R. G., and Case, J. E., 1975. Geophysical studies in the Gulf of Mexico. *In* Nairn, A. E. M., and Stehli, F. G. (Eds.), *The Ocean Basin and Margins* (Vol. 3): New York (Plenum Press), 65–105.

Moore, T. C., Jr., Rabinowitz, P. D., et al., in press. *Init. Repts. DSDP*, 74: Washington (U.S. Govt. Printing Office).

Roggenthen, W. M., and Napoleone, G., 1977. Upper Cretaceous–Paleocene magnetic stratigraphy at Gubbio, Italy. IV. Upper Maestrichtian–Paleocene magnetic stratigraphy. *Geol. Soc. Am. Bull.*, 88:378–382.

Tucholke, B. E., Vogt, P. R., et al., 1979. *Init. Repts. DSDP*, 43: Washington (U.S. Govt. Printing Office).

Worzel, J. L., Bryant, W., et al., 1973. *Init. Repts. DSDP*, 10: Washington (U.S. Govt. Printing Office).

Date of Initial Receipt: July 5, 1983
Date of Acceptance: July 6, 1983

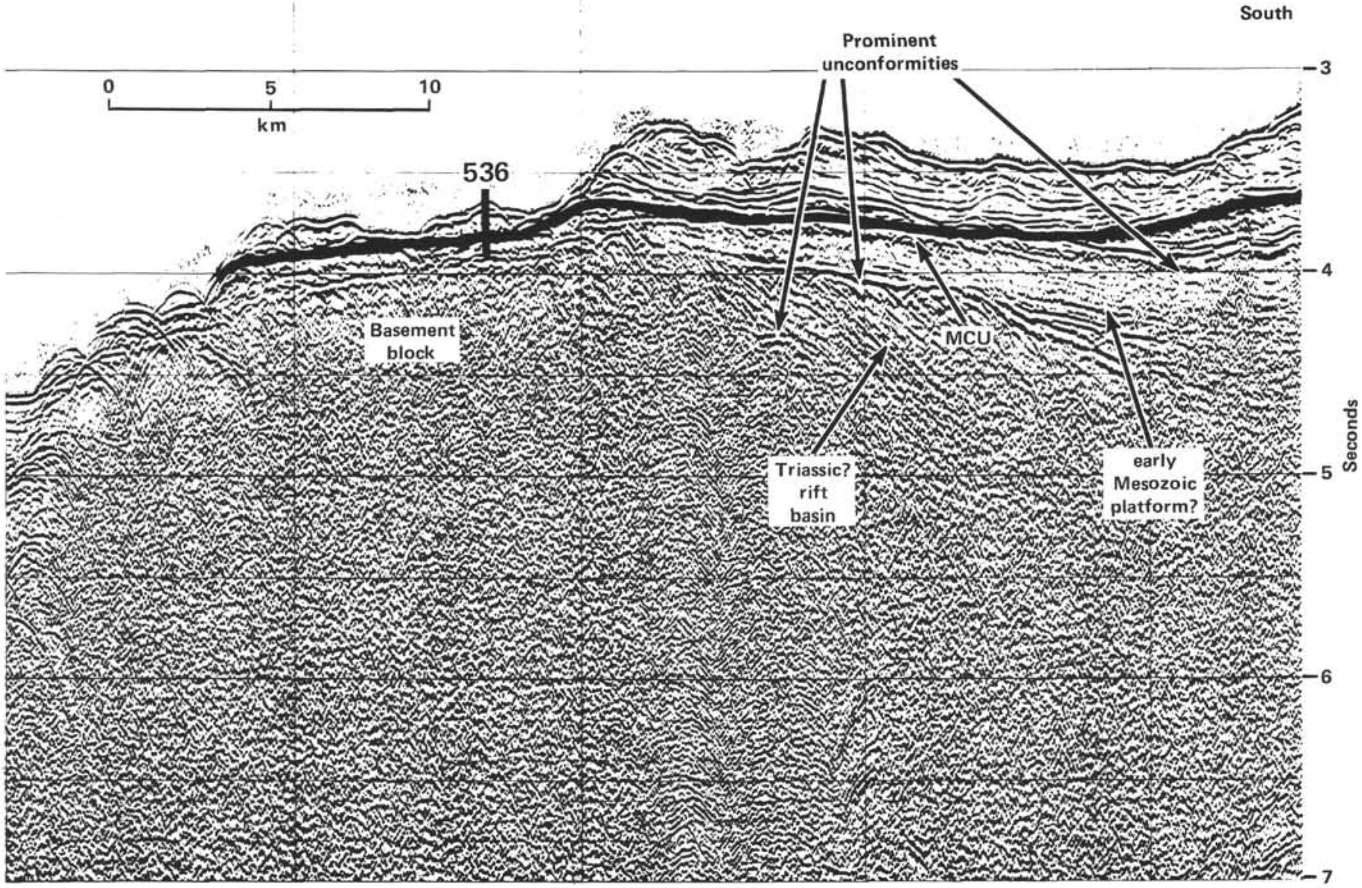

Figure 13. Closeup of seismic reflection Line GT3-75 (Fig. 3) showing details of seismic stratigraphy at Site 536. MCU = mid-Cretaceous unconformity.

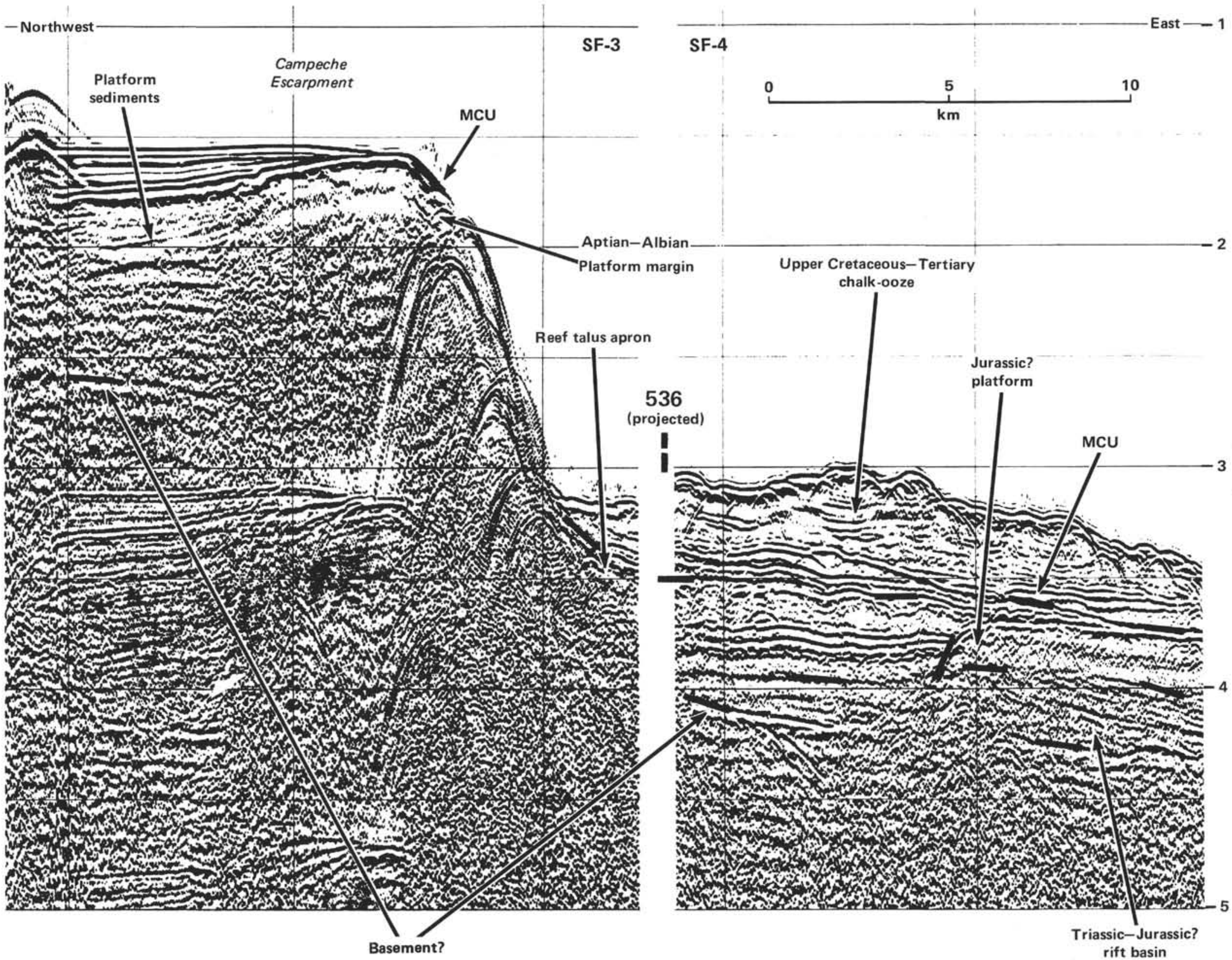

Figure 14. Interpretation of seismic Lines SF-3 and SF-4 across Campeche Escarpment just southeast of Site 536 based on drilling results. MCU = mid-Cretaceous unconformity. See Figure 1 for location of line.

SITE 536 HOLE CORE 1 CORED INTERVAL 0.0–4.0 m

TIME – ROCK UNIT: Pleistocene
BIOSTRATIGRAPHIC ZONE: *Globorotalia truncatulinoides* N22 (F); *Emiliania huxleyi* CN15
FOSSIL CHARACTER: FORAMINIFERS AG; NANNOFOSSILS AG
SECTION: 1, 2, 3, CC
METERS: 0.5, 1.0

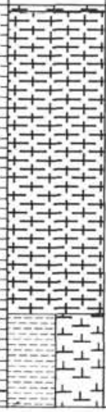

LITHOLOGIC DESCRIPTION

MARLY NANNOFOSSIL OOZE and FORAMINIFERAL-NANNOFOSSIL OOZE, variable colors and extreme drilling deformation. In Section 1 sediment changes from very light gray (N8) nannofossil ooze to moderate yellowish brown (10YR 5/4) foraminiferal-nannofossil ooze at ~6 cm then to light olive gray (5Y 4/1) foraminiferal nannofossil ooze with indistinct medium ,gray (N5) bands and streaks. In Section 2 this ooze is pale yellowish brown (10YR 6/2) to 50 cm, then very light gray (N8) with pale yellowish brown mottling. A grayish blue (5PB 5/2) layer at ~76 cm is glauconitic. Foraminiferal nannofossil ooze changes to very light gray then light olive gray (5Y 6/1) nannofossil ooze with grayish green bands (10GY 5/2). Diatoms noted in smear slides from this section.

SMEAR SLIDE SUMMARY (%):

	1, 3 M	1, 31 D	2, 76 M	2, 148 D	3, 13 D	3, 39 M	CC D
Texture:							
Sand	–	–	–	–	–	5	–
Silt	–	30	20	20	10	15	–
Clay	–	70	80	80	90	80	–
Composition:							
Quartz	–	–	–	–	–	–	2
Mica	5	–	–	–	–	–	3
Clay	10	20	10	10	10	25	15
Glauconite	–	–	2	Tr	–	–	–
Carbonate unspec.	10	10	–	5	2	10	10
Foraminifers	30	30	17	10	8	5	10
Calc. nannofossils	30	40	70	74	80	60	58
Diatoms	–	–	–	–	–	10	5
Sponge spicules	5	Tr	1	1	Tr	–	1
Fish remains	3	–	–	–	–	–	–
Pteropod fragments	5	–	–	–	–	–	–
Tunicate spicules	2	Tr	Tr	Tr	Tr	Tr	1

ORGANIC CARBON AND CARBONATE (%):

	2, 40	2, 60	3, 48	3, 60
Organic carbon	–	–	–	–
Carbonate	64	70	44	53

SITE 536 HOLE CORE 2 CORED INTERVAL 4.0–13.5 m

TIME – ROCK UNIT: late Pleistocene; early Pliocene
BIOSTRATIGRAPHIC ZONE: *Emiliania huxleyi* CN15; *Globorotalia margaritae* zone, *Amaurolithus tricorniculatus* CN10
FOSSIL CHARACTER: NANNOFOSSILS AG; FORAMINIFERS AG, NANNOFOSSILS AG
SECTION: 1, 2, CC
METERS: 0.5, 1.0

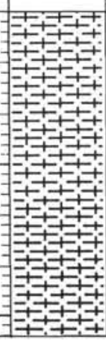

LITHOLOGIC DESCRIPTION

FORAMINIFERAL-NANNOFOSSIL OOZE, banded very light gray (N8), light gray (N7) to light olive gray (5Y 6/1), light brownish gray (5YR 6/1), and pale yellowish brown (10YR 6/2). Deformed thin bands and patches of medium gray (N5) to dusky blue (5PB 3/2) (Section 1) and grayish blue (5PB 5/2) (Section 2) also occur. Moderate to extreme drilling deformation.

SMEAR SLIDE SUMMARY (%):

	1, 120 D	2, 60 M	2, 120 D
Texture:			
Sand	10	10	10
Silt	10	10	10
Clay	80	80	80
Composition:			
Clay	5	10	5
Glauconite	–	Tr	–
Carbonate unspec.	5	5	2
Foraminifers	10	10	13
Calc. nannofossils	80	80	80
Tunicate spicules	Tr	–	–

ORGANIC CARBON AND CARBONATE (%):

	2, 4
Organic carbon	–
Carbonate	69

SITE 536 HOLE CORE 3 CORED INTERVAL 13.5–23.0 m

TIME – ROCK UNIT: early Pliocene
BIOSTRATIGRAPHIC ZONE: *Globorotalia margaritae* zone, *Amaurolithus tricorniculatus* CN10
FOSSIL CHARACTER: FORAMINIFERS AM; NANNOFOSSILS AG
SECTION: 1, 2, 3, 4, 5, 6, CC
METERS: 0.5, 1.0
SAMPLES: IW, OG

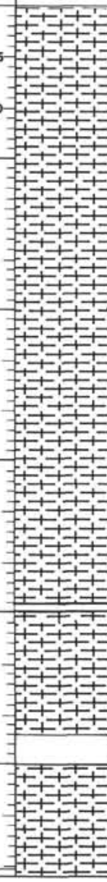

LITHOLOGIC DESCRIPTION

FORAMINIFERAL-NANNOFOSSIL OOZE, very light gray (N8) to light gray (N7) with a very pale blue (5B 8/2) tint. Streaks of grayish blue (5PB 5/2) and irregular yellowish gray (5Y 7/2) to grayish yellow green (5GY 7/2) patches and streaks occur throughout.

SMEAR SLIDE SUMMARY (%):

	2, 50 D
Texture:	
Sand	10
Silt	5
Clay	85
Composition:	
Clay	5
Carbonate unspec.	2
Foraminifers	10
Calc. nannofossils	83
Diatoms	–
Dolomite(?)	–

ORGANIC CARBON AND CARBONATE (%):

	3, 80
Organic carbon	–
Carbonate	71

SITE 536 HOLE CORE 4 CORED INTERVAL 23.0–32.5 m

TIME-ROCK UNIT: middle Miocene

BIOSTRATIGRAPHIC ZONE: *Discoaster quinqueramus* N9 (F); *Globorotalia acostaensis* N17 (F)

FOSSIL CHARACTER (FORAMINIFERS, NANNOFOSSILS, RADIOLARIANS, DIATOMS): AG; AG; AM AG

SECTION: 1, 2, 3, 4, CC — METERS: 0.5, 1.0

GRAPHIC LITHOLOGY / DRILLING DISTURBANCE / SEDIMENTARY STRUCTURES / SAMPLES

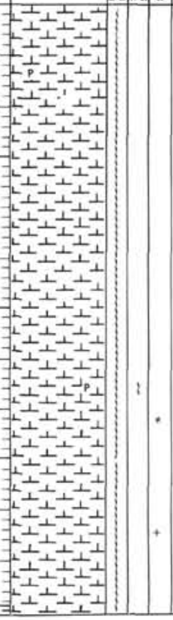

LITHOLOGIC DESCRIPTION

NANNOFOSSIL OOZE, very light gray (N8) to light gray (N7) with a very pale blue (5B 8/2) tint. Grayish blue (5PB 5/2) streaks and spots and irregular patches of yellowish gray (5Y 7/2) to grayish yellow green (5GY 7/2) common. Small olive black (5Y 2/1) pyrite patch at 65 cm, Section 1. Several small (1–2 cm long), hard pyritized burrows at 80 cm, Section 3.

SMEAR SLIDE SUMMARY (%):

	3, 110
	D
Texture:	
Sand	3
Silt	30
Clay	67
Composition:	
Clay	10
Carbonate unspec.	3
Foraminifers	5
Calc. nannofossils	77
Diatoms	5
Dolomite(?)	Tr

ORGANIC CARBON AND CARBONATE (%):

	4, 77
Organic carbon	–
Carbonate	75

SITE 536 HOLE CORE 5 CORED INTERVAL 32.5–42.0 m

TIME-ROCK UNIT: middle Miocene

BIOSTRATIGRAPHIC ZONE: *Globorotalia acostaensis* N16; *Discoaster quinqueramus* N9

FOSSIL CHARACTER: FM AG

SECTION: 1, 2, CC — METERS: 0.5, 1.0

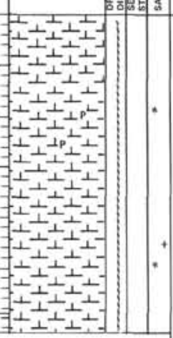

LITHOLOGIC DESCRIPTION

NANNOFOSSIL OOZE, light greenish gray (5GY 8/1) with scattered light olive gray (5Y 4/1) patches and mottling. No obvious compositional differences between patches and principal lithology. Streaky pyrite patches at 104–120 cm, Section 1.

SMEAR SLIDE SUMMARY (%):

	1, 96	2, 96
	M	D
Texture:		
Sand	2	–
Silt	18	5
Clay	80	95
Composition:		
Clay	5	2
Carbonate unspec.	–	5
Foraminifers	8	5
Calc. nannofossils	87	88
Dolomite(?)	Tr	–

ORGANIC CARBON AND CARBONATE (%):

	2, 76
Organic carbon	–
Carbonate	75

SITE 536 HOLE CORE 6 CORED INTERVAL 42.0–51.5 m

TIME-ROCK UNIT: middle Miocene

BIOSTRATIGRAPHIC ZONE: *Globorotalia acostaensis* N16 (F); *Discoaster exilis* CN5 (N)

FOSSIL CHARACTER: AG; AG AG

SECTION: 1, 2 — METERS: 0.5, 1.0

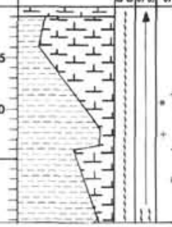

LITHOLOGIC DESCRIPTION

NANNOFOSSIL OOZE grading to MARLY NANNOFOSSIL OOZE and NANNOFOSSIL CLAY in two apparent sequences. Top 10 cm, Section 1, is mottled light greenish gray (5GY 8/1) ooze. Sharp drilling contact separates this from marly ooze below. This grades from ooze to marly ooze to greenish gray (5G 5/2) clay at 126–130 cm of Section 1. Relatively sharp change back to light greenish gray ooze may be drilling contact. Sediment grades back to grayish green clay at ~45 cm in Section 2. Burrows are common in all lithologies but deformed by drilling. Burrows filled with minor lithology and color contrasts are great with host lithology. Some yellowish gray (5Y 8/1) mottling throughout.

SMEAR SLIDE SUMMARY (%):

	1, 99	2, 23
	D	D
Texture:		
Sand	1	2
Silt	30	80
Clay	69	18
Composition:		
Quartz	Tr	Tr
Heavy minerals (hornblende)	–	Tr
Clay	75	15
Volcanic glass	Tr	–
Carbonate unspec.	1	1
Foraminifers	–	1
Calc. nannofossils	24	83
Dolomite(?)	Tr	Tr

ORGANIC CARBON AND CARBONATE (%):

	1, 86	1, 123	1, 140
Organic carbon	–	–	–
Carbonate	35	19	45

SITE 536 HOLE CORE 7 CORED INTERVAL 51.5–61.0 m

TIME-ROCK UNIT: early Miocene

BIOSTRATIGRAPHIC ZONE: *Globorotalia fohsi* zone N10–11 (F); *Sphenolithus heteromorphus* CN4 (N)

FOSSIL CHARACTER: AG; AG AG

SECTION: 1, 2, 3, CC — METERS: 0.5, 1.0

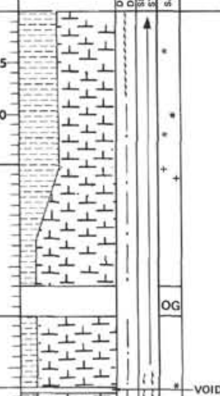

LITHOLOGIC DESCRIPTION

NANNOFOSSIL OOZE to MARLY NANNOFOSSIL OOZE, light greenish gray (5GY 8/1) with abundant and variable color mottling. Light olive (5Y 5/2) patches near top Section 1 are diatom-rich. Dark gray (N3) and medium dark gray (N4) patches contain pyrite and some siliceous microfossils. Grayish green (10GY 5/2) patches are glauconitic. Sponge spicules occur in all smear slides examined.

SMEAR SLIDE SUMMARY (%):

	1, 41	1, 103	1, 120	3, 70
	M	M	D	D
Texture:				
Sand	5	Tr	10	10
Silt	80	70	70	70
Clay	15	30	20	20
Composition:				
Clay	15	20	20	20
Volcanic glass	–	Tr	Tr	–
Pyrite	1	35	–	–
Foraminifers	7	10	5	15
Calc. nannofossils	58	30	73	60
Diatoms	15	–	–	Tr
Radiolarians	Tr	–	–	1
Sponge spicules	5	5	2	5
Silicoflagellates	Tr	–	–	–

ORGANIC CARBON AND CARBONATE (%):

	2, 9	2 118
Organic carbon	–	–
Carbonate	57	77

SITE 536 HOLE CORE 8 CORED INTERVAL 61.0–70.5 m

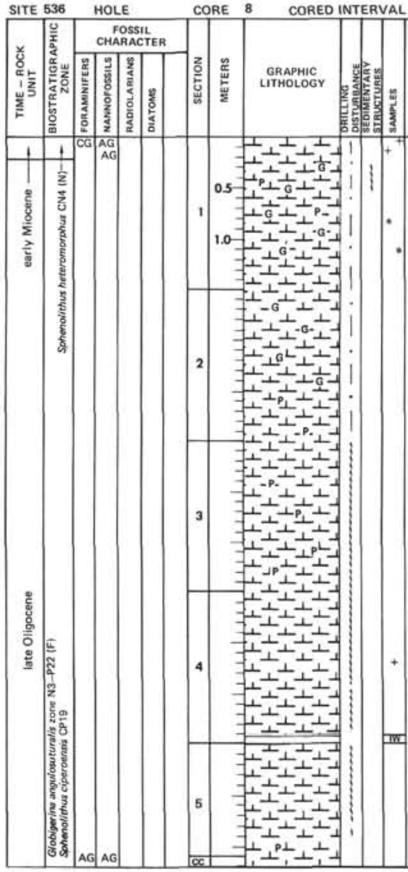

LITHOLOGIC DESCRIPTION

NANNOFOSSIL OOZE, changing from light bluish gray (5B 7/1) ooze to homogeneous yellowish gray (5Y 8/1) to white (N9) ooze across a sharp contact at 7–10 cm in Section 1. Scattered glauconite-rich patches in first two sections give way to pyrite patches below. Pyrite fades out below Section 3. Semi-lithified pieces of ooze occur in Sections 4 and 5.

SMEAR SLIDE SUMMARY (%):

	1, 83 M	1, 110 D
Texture:		
Sand	30	–
Silt	70	95
Clay	–	5
Composition:		
Clay	–	5
Glauconite	50	–
Foraminifers	10	3
Calc. nannofossils	40	92
Radiolarians	Tr	–

ORGANIC CARBON AND CARBONATE (%):

	1, 4	1, 13	4, 70
Organic carbon	–	–	–
Carbonate	73	82	83

SITE 536 HOLE CORE 9 CORED INTERVAL 70.5–80.0 m

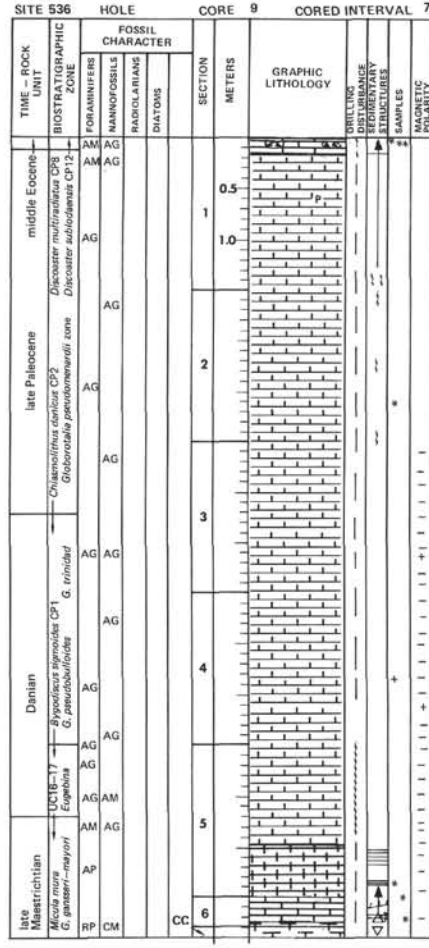

LITHOLOGIC DESCRIPTION

NANNOFOSSIL CHALK, homogeneous grayish orange (10YR 7/4) changing downcore to mottled grayish orange pink (5YR 7/2–10YR 8/2) with yellowish brown (10YR 5/4) mottles and very pale orange (10YR 8/2). Medium gray pyrite patches are common. Top 3 cm of Section 1 is white LIMESTONE; pieces just below this at 3–15 cm are dark yellowish brown opal-CT CHERT and yellowish gray (5Y 8/1) SILICEOUS LIMESTONE. At ~ 95 cm in Section 5 foraminifer-rich patches become common in chalk. Dispersed foraminifers also are present in the chalk in amounts great enough to term it a FORAMINIFERAL NANNOFOSSIL CHALK. Graded, laminated, and cross-laminated LIMESTONE. Composed principally of foraminifers and clay (spherulitic) cemented by calcite occurs at base Section 5 top Section 6. At base of Section 6 (the coarse part of this layer) the sediment is an unlithified FORAMINIFERAL OOZE that appears to be reversely graded. Abundant pteropod debris occurs at base of Core-Catcher in the foraminifer ooze.

Thin Sections:

1, 1: Foraminiferal limestone (mudstone) – principally micrite (65%), scattered foraminifers (30%), and clay (5%).

1, 8: Foraminiferal limestone (mudstone) – same as Section 1, 1 cm.

6, 3: Foraminiferal limestone (grainstone) – consists of 10%(?) foraminifers and 10% lithoclasts in sparry calcite (50%), and cement. Lithoclasts are rounded elements of micrite, well-sorted in range (0.300 mm). Traces of metamorphic slate (1 or 2 grains). Cement is mostly blocky calcite but clay is also present in concretionary zones and rims round debris.

SMEAR SLIDE SUMMARY (%):

	1, 8 D	2, 110 D	5, 139 M	6, 26 M
Texture:				
Sand	–	–	4	7
Silt	–	95	11	15
Clay	–	5	85	78
Composition:				
Quartz	–	–	Tr	Tr
Feldspar	–	–	Tr	Tr
Clay	5	85	10(?)	5
Carbonate unspec.	15	–	13	5
Foraminifers	20	–	Tr	Tr
Calc. nannofossils	60	95	Tr	Tr
Dolomite	–	–	2	–
Tunicate spicules	–	–	Tr	–
Calcispheres	–	–	–	Tr

ORGANIC CARBON AND CARBONATE (%):

	4, 81
Organic carbon	–
Carbonate	86

SITE 536 HOLE CORE 10 CORED INTERVAL 80.0–89.5 m

TIME – ROCK UNIT	BIOSTRATIGRAPHIC ZONE	FORAMINIFERS	NANNOFOSSILS	RADIOLARIANS	DIATOMS	SECTION	METERS	GRAPHIC LITHOLOGY	DRILLING DISTURBANCE	SEDIMENTARY STRUCTURES	SAMPLES
		RP RP RP				1	0.5	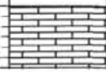	△ △ △		* * * * *

LITHOLOGIC DESCRIPTION

LIMESTONE (grainstone), white (N9), consisting of broken drilling fragments of moderately well-sorted to very poorly sorted grainstones. Largest skeletal fragment (rudist) is up to diameter of core (5 cm). Skeletal debris includes rudist fragments (one large radiolitid), coral fragments, other bivalves, gastropods, foraminifers, and echinoderm fragments. Medium light gray (N6) to dark gray (N3) skeletal debris occurs between 20–60 cm. All pieces have been leached and have excellent primary and secondary porosity.
(Note: spacers put between fragments for shipping gives greater length of recovered material in graphic lithology column.).

Thin Sections:

1, 2: Limestone (skeletal grainstone) – well-sorted, containing well-rounded skeletal fragments of molluscs (50%), echinoderms (5%) and coral (5%) with some unidentified clasts (10%; one limestone lithoclast). Cement is micrite (30%). Good primary and moldic porosity. Secondary porosity rimmed with scale-euhedral drusy calcite crystals (< 10 μm). Micritic rims on most pores. Some primary pores filled with dark, fine-grained material.

1, 5: Limestone (skeletal packstone-wackestone) – fine-grained and porous consisting of skeletal debris of molluscs, foraminifers and echinoderms and pelloids in a micritic matrix.

1, 38: Limestone (skeletal grainstone) – sample consists of skeletal debris (64%), limestone lithoclasts (15%), cement (20%), and pyrite (1%). Skeletal fragments are bivalves (75%; rudists), echinoderms (5%), and coral, green and red algae plus unidentified grains (18%). Coated grains also occur (2%). Sorting is poor, fragments are rounded, sometimes coated and bored. Lithoclasts are dark micrite or recrystallized micrite or biomicrite. Cement is drusy calcite or microsparite.

1, 43: Limestone (skeletal grainstone) – poorly sorted and rounded skeletal debris (80%) cemented by microspar or drusy calcite. Skeletal grains include rudists and other bivalves (60%), echinoderms (10%), bryozoans (5%), coated grains (15%), and assorted foraminifers, coral, algae, gastropods (10%). Micritic envelopes common. Some lithoclasts. Good porosity with dark material filling some primary pores.

1, 47: Limestone (skeletal grainstone) – contains molluscs (50%), micrite grains (10%), green algae (5%), red algae (5%), echinoderms (5%), lithoclasts (5%), and unidentified grains (20%). Leached, with good primary and secondary porosity. Fringes of calcite cement (~10μm crystals) around grains and pores; dark material in some primary pores succeeds calcite cement. Grain size ranges from 1 mm up; common micritic envelopes.

SITE 536 HOLE CORE 11 CORED INTERVAL 89.5–99.0 m

TIME – ROCK UNIT	BIOSTRATIGRAPHIC ZONE	FORAMINIFERS	NANNOFOSSILS	RADIOLARIANS	DIATOMS	SECTION	METERS	GRAPHIC LITHOLOGY	DRILLING DISTURBANCE	SEDIMENTARY STRUCTURES	SAMPLES
Albian (Vraconian)	*Planomalina buxtorfi* zone LC19	FM				CC		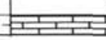	△		*

LITHOLOGIC DESCRIPTION

LIMESTONE (skeletal wackestones and grainstones), white (N9), consisting of poorly sorted skeletal debris. Several pieces have secondary moldic porosity developed; pores lined with calcite crystals and drusy cement. Piece at 18 cm is part of a rudist (caprinid). Core consists of drilling breccia.

Thin Section:

1, 13: Limestone (skeletal grainstone) – skeletal debris (30%) and micrite lithoclasts (10%) in microspar and drusy calcite cement (60%). Skeletal debris is rounded and poorly sorted and includes bivalves (45%), echinoderms (45%), and bryozoans, foraminifers, and algae (10%). Micritic rims on grains common.

SITE 536 HOLE CORE 12 CORED INTERVAL 99.0–108.5 m

TIME – ROCK UNIT	BIOSTRATIGRAPHIC ZONE	FORAMINIFERS	NANNOFOSSILS	RADIOLARIANS	DIATOMS	SECTION	METERS	GRAPHIC LITHOLOGY	DRILLING DISTURBANCE	SEDIMENTARY STRUCTURES	SAMPLES
Comanchean lower Cretaceous			RP			CC			△		

LITHOLOGIC DESCRIPTION

LIMESTONE (skeletal grainstone and wackestone), light gray (N7) to white (N9). Largest piece is a rudist grainstone to wackestone with geopetal lime mudstone filling cavities; rudists in this piece probably *Eoradiolites* sp. Other pieces are grainstones with one possible lithoclast. Drilling breccia.

SITE 536 HOLE CORE 13 CORED INTERVAL 108.5–118.0 m

TIME – ROCK UNIT	BIOSTRATIGRAPHIC ZONE	FORAMINIFERS	NANNOFOSSILS	RADIOLARIANS	DIATOMS	SECTION	METERS	GRAPHIC LITHOLOGY	DRILLING DISTURBANCE	SEDIMENTARY STRUCTURES	SAMPLES
Comanchean–lower Cretaceous		RP RP				1	0.5	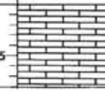	△ △ △ △		* *

LITHOLOGIC DESCRIPTION

LIMESTONE (skeletal grainstone), white (N9), skeletal fragments consisting of rudists, gastropods, other molluscs, corals, and medium gray (N5) grains. Coarser material is primarily mollusc debris which is leached to produce moldic secondary porosity. Primary porosity also present. Core is drilling breccia (length of recovered material greater than true because of spacers in half liner).

Thin Sections:

1, 39: Limestone (skeletal grainstone) – poorly sorted consisting of rounded skeletal fragments (30%), micritized grains (20%), peloids (10%), and microspar cement (50%). Well developed secondary moldic porosity; many skeletal fragments completely dissolved leaving only microspar-coated micritic envelopes. Grain size medium to coarse sand.

1, 68: Limestone (skeletal grainstone) – poorly sorted with rounded skeletal fragments (70%) and interstitial microspar cement (30%). Skeletal grains include molluscs (30%), echinoderms (5%), gastropods (1%), rudists (5%), coral (5%), and unidentified spar-replaced grains with micritic envelopes (29%). Many grains have micritic envelopes and spar or microspar interiors. Porosity is mainly primary interparticle porosity though secondary moldic porosity is also present.

SITE 536 HOLE CORE 14 CORED INTERVAL 118.0–127.5 m

TIME – ROCK UNIT	BIOSTRATIGRAPHIC ZONE	FORAMINIFERS	NANNOFOSSILS	RADIOLARIANS	DIATOMS	SECTION	METERS
Comanchean–lower Cretaceous		RP				1	0.5

LITHOLOGIC DESCRIPTION

LIMESTONE (skeletal grainstone), white (N9), consisting of coarse skeletal debris of the same type as Cores 10–13. Several medium-grained carbonate "sandstone" layers in well-cemented limestone pieces dip ~ 15° . Porous with excellent secondary porosity. Core is drilling breccia near base (spacers inserted, so length of recovered material is exaggerated).

Thin Sections:

1, 21: Limestone (skeletal grainstone) – poorly sorted grainstone with rounded skeletal and micritized grains (70%) and interparticle microspar cement (30%). Skeletal grains include molluscs (40%), rudists (5%), and echinoderms (5%); micritized grains, including some peloids, amount to ~ 20%. All grains have micritic envelopes; centers of most grains replaced by microspar. Dark, very fine-grained material fills and replaces parts of grains. Some primary porosity but most is secondary moldic porosity.

1, 56: Limestone (skeletal grainstone) – consists of about 40% microspar cement, 60% grains. Very poorly sorted. Skeletal grains include molluscs (30%), rudists (2%), coral (2%), algae (2%), echinoderms (1%), and foraminifers (Tr); micritized and replaced grains amount to about 20%. Grains are subrounded. Primary porosity about equal to secondary moldic porosity. Very dark micrite replaces parts of many grains.

SITE 536 HOLE CORE 15 CORED INTERVAL 127.5–137.0 m

TIME – ROCK UNIT	BIOSTRATIGRAPHIC ZONE	FORAMINIFERS	NANNOFOSSILS	RADIOLARIANS	DIATOMS	SECTION	METERS
Comanchean–lower Cretaceous		RP				1	

LITHOLOGIC DESCRIPTION

LIMESTONE (skeletal grainstone), white (N9), well-cemented with drusy calcite. Coarse skeletal material present. Fragments include coral, rudists, gastropods, molluscs, and foraminifers. Sand-size gray (N7) grains in piece at 20 cm. Two pieces at 34 cm are laminated mudstones containing spherical microfossil molds. Core is drilling breccia. (Spacers inserted in half liner exaggerates recovered length).

Thin Section:

1, 31: Limestone (mudstone) – limestone composed principally of dark and light patches of micrite with abundant secondary moldic porosity. Molds are mainly round and rectangular (~0.1–0.5 mm), probably dissolved radiolaria, foraminifers, and shell debris. Reddish brown coatings and partial fills of some pores. Rectangular molds often parallel to bedding.

SITE 536 HOLE CORE 16 CORED INTERVAL 137.0–146.5 m

TIME – ROCK UNIT	BIOSTRATIGRAPHIC ZONE	FORAMINIFERS	NANNOFOSSILS	RADIOLARIANS	DIATOMS	SECTION	METERS
upper Aptian	*Hedbergella gorbachikae* zone	RP, RP, RP, RP				1	0.5

LITHOLOGIC DESCRIPTION

LIMESTONE (skeletal grainstone and wackestone), white (N9), containing skeletal fragments up to 3 cm across. Piece at 55 cm is part of a radiolitid rudist wall. Piece at 60 cm is a well-laminated mudstone containing spherical microfossils and possible ammonites. Core is drilling breccia. (Spacers in core liner exaggerate core length.)

Thin Sections:

1, 1: Limestone (skeletal wackestone) – consists principally of dark micrite between grains (pores) and light, slightly coarser grained micrite around grains. Grains (30%) which are preserved include several large 1–3 mm fragments of rudists, molluscs and echinoderms. Most "grains" are smaller (0.1–1.0 mm) and completely dissolved to form irregular secondary moldic porosity. No good micritic envelopes with microspar crusts in pores. Darker micrite replaces parts of a few mollusc fragments.

1, 27: Limestone (mudstone) – mostly dark micrite grading to slightly lighter and coarser grained micrite bordering pores. No grains in sample; all have been dissolved to form secondary moldic porosity. Pores are ~0.2 mm across and round (foraminifer and/or radiolaria molds). Some molds (~0.2–0.5 mm) are probably small shell fragments.

1, 38: Limestone (skeletal wackestone to mudstone) – dominantly light and dark micrite with scattered, partly replaces shell debris and ghosts of others in micrite. Shell debris is mostly ~ 0.2 mm but several large partly replaced rudist fragments present. Some large rudist fragments are completely dissolved leaving only interval and external molds.

1, 56: Limestone (mudstone) – 100% light and dark micrite intermixed in blotchy pattern with abundant (0.3–0.5 mm) subround or oval microfossil molds. Molds have thin coatings of microspar.

SITE 536 HOLE CORE 17 CORED INTERVAL 146.5–156.0 m

TIME – ROCK UNIT	BIOSTRATIGRAPHIC ZONE	FORAMINIFERS	NANNOFOSSILS	RADIOLARIANS	DIATOMS	SECTION	METERS
lower Cretaceous		RP				1	

LITHOLOGIC DESCRIPTION

LIMESTONE (skeletal grainstone and wackestone), white (N9), well-cemented, leached with rare gray grains at 20–30 cm. Piece at 5 cm has a thin (1 cm) mudstone layer. Core is a drilling breccia. (Spacers in core liner result in exaggerated recovered core length.)

Thin Section:

1, 5: Limestone (skeletal[?] wackestone) – wackestone with two packstone zones or layers. Wackestone is mostly dark micrite with small (0.05–0.3 mm) microspar patches (replaced radiolaria[?], foraminifers and some flat shell layers). Many microfossils completely dissolved to give moldic porosity. Packstone has grains with micritic envelopes, microspar interiors or completely dissolved interiors (secondary moldic porosity).

SITE 536 HOLE CORE 18 CORED INTERVAL 156.5–165.5 m

TIME – ROCK UNIT	BIOSTRATIGRAPHIC ZONE	FORAMINIFERS	NANNOFOSSILS	RADIOLARIANS	DIATOMS	SECTION	METERS	GRAPHIC LITHOLOGY	DRILLING DISTURBANCE	SEDIMENTARY STRUCTURES	SAMPLES
late Aptian		RP				1		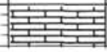	△ △		*

LITHOLOGIC DESCRIPTION

LIMESTONE (skeletal grainstone), white (N9), with fine to coarse skeletal debris including fragments of corals, rudists, gastropods, and some foraminifers. Core consists of drilling breccia fragments. Most pieces are well-cemented grainstones. Several pieces (at 20, 32, and 37 cm) are mudstones with scattered spherical, spar-filled microfossils. One piece (37 cm) has a coarser grained band ~1 cm thick. (Spacers in core half liner exaggerate core length.)

Thin Section:

1, 40: Limestone (mudstone with grainstone layers) – mudstone is mostly dark micrite with microspar-filled microfossils. Unfilled molds give secondary porosity. Grainstone contains flay-lying mollusc fragments, foraminifers, and unidentified peloidal fragments. Many are micritized. Grains are spar and microspar.

SITE 536 HOLE CORE 19 CORED INTERVAL 165.5–175.0 m

TIME – ROCK UNIT	BIOSTRATIGRAPHIC ZONE	FORAMINIFERS	NANNOFOSSILS	RADIOLARIANS	DIATOMS	SECTION	METERS	GRAPHIC LITHOLOGY	DRILLING DISTURBANCE	SEDIMENTARY STRUCTURES	SAMPLES
late Aptian?	*Globigerinelloides algerianus* ?	RP RP				1		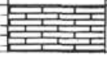	△ △		*

LITHOLOGIC DESCRIPTION

LIMESTONE (skeletal grainstone and mudstone), white (N9) (grainstone) and yellowish gray (5Y 8/1) (mudstone); mudstones are homogeneous with rare spherical microfossil molds. Grainstones contain skeletal debris. No large rudist or coral fragments as in Cores 10–17. Core is drilling breccia. (Spacers in core half liner exaggerate length of recovered material.)

Thin Section:

1, 3: Limestone (mudstone) – core is 80% micrite, 20% microspar (filled microfossils). Light and dark micrite with one irregular sharp boundary between the two; remaining is blotchy mixture. Microfossils are ~0.02–0.3 mm across and mostly filled with microspar. Most look like replaced and filled radiolaria, foraminifers, and mollusc fragments. Sparse moldic porosity.

SITE 536 HOLE CORE 20 CORED INTERVAL 175.0–184.5 m

TIME – ROCK UNIT	BIOSTRATIGRAPHIC ZONE	FORAMINIFERS	NANNOFOSSILS	RADIOLARIANS	DIATOMS	SECTION	METERS	GRAPHIC LITHOLOGY	DRILLING DISTURBANCE	SEDIMENTARY STRUCTURES	SAMPLES
lower Cretaceous		FP				1			△		* * * *

LITHOLOGIC DESCRIPTION

LIMESTONE (skeletal grainstone and mudstone), very pale orange (10YR 8/2) (mudstone), white (N9) and light gray (N7) (grainstones); one piece is an oolitic grainstone discolored by fine-grained dark material disseminated throughout. Two other pieces stained with iron-oxides and/or manganese oxides and appear weathered. Core is drilling debris. (Spacers in core half liner exaggerate length of recovered material.)

Thin Sections:

1, 2: Limestone (mudstone) – sample consists principally of dark micrite (45%) grading to microspar near voids and pores, about 10% echinoid spines and 5% mollusc fragments. Sorting is moderate. Porosity is ~40%, mostly moldic secondary porosity. Most skeletal fragments have been completely dissolved.

1, 10: Pisolitic limestone (grainstone) – about 70% grains, 30% sparry cement. Grains include coated grains (40%), fragments of echinoderms (10%), molluscs (1%) and gastropods (1%), and foraminifers (18%). Coated grains mostly have echinoderm cores with concentric coatings. Limestone lithoclasts and gastropods also comprise cores of pisolites. Some cores of pisolites completely dissolved leaving only concentric outer layers. Echinoderm and mollusc fragments most common other non-coated grains; all are micritized. Small mollusc fragments have micritic rims and coarser microspar/spar recrystallized interiors. Most porosity is secondary moldic porosity.

1, 20: Limestone (mudstone) – mostly micrite (50%) and microspar (25%), the latter lining voids. Porosity (~ 25%) is moldic, principally 0.1–0.2 mm circular spaces with rare elongate (shell) voids.

1, 24: Limestone (skeletal packstone) – sample consists of about 30% micrite, 20% skeletal fragments, 15% foraminifers, 15% microspar, and traces of gastropods, ooids, and echinoderms. Porosity is ~20% and mostly secondary moldic type. Some packed grains have been replaced by spar. Grainsize ≅ 0.1–0.2 mm

SITE 536 HOLE CORE 21 CORED INTERVAL 184.5–194.0 m

TIME – ROCK UNIT	BIOSTRATIGRAPHIC ZONE	FORAMINIFERS	NANNOFOSSILS	RADIOLARIANS	DIATOMS	SECTION	METERS	GRAPHIC LITHOLOGY	DRILLING DISTURBANCE	SEDIMENTARY STRUCTURES	SAMPLES
late Aptian		CM				1 2	0.5 1.0	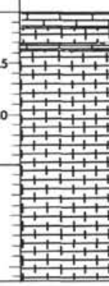			* * *

LITHOLOGIC DESCRIPTION

LIMESTONE and DOLOMITE. Limestone is white (N9) to light gray (N8) and occurs as several small broken pieces in Section 1 and contains subrounded fine to coarse sand-size skeletal debris. Dolomite is mottled pale yellowish brown (10YR 6/2) to moderate and dark yellowish brown (10YR 5/4–10YR 4/2) with some dark yellowish orange (10YR 6/6) staining. Dolomite is massive and finely crystalline for the most part and shows some indistinct layering in a few pieces (e.g. 60 and 125 cm, Section 1), but more commonly an indistinct blotchy color mottling. Large (1 cm x 3 mm), flattened and open pores (fenestral or birds-eye-like porosity) are common between 75–85 cm, Section 1. X-ray diffraction of piece at 72 cm, Section 2 confirms composition as dolomite. (Note: during drilling of core drillers report momentary loss of weight and rapid penetration of ~ 5 m suggesting cavernous porosity may be present.)

Thin Sections:

1, 32: Limestone (mudstone) – principally light and dark micrite (50%) with abundant round and platy microfossil molds (~ 50%), 0.1–0.4 mm across. Most molds are filled with spar and microspar. Sizes and shapes suggest replaced radiolaria, foraminifers, and filaments. One large (1–2 mm) mollusc fragment has been completely dissolved. Some microfossil molds are empty, but porosity of this type is low.

1, 126. Dolomite – fine- to medium-grained dolomite composed of interlocking rhombic crystals with dark material along edges and faces. Reddish yellow staining around some pore spaces. Pores are sparse and irregular; possibly fossil molds. Layering in this sample derives from zones of fine (5–10 μm) and coarser (40–50 μm) dolomite.

2, 62: Dolomite – same as Section 1, 126 cm. Abundant (0.2–2.0 mm) irregular pores.

SITE 536 HOLE CORE 22 CORED INTERVAL 194.0–203.5 m

TIME – ROCK UNIT	BIOSTRATIGRAPHIC ZONE	FOSSIL CHARACTER: FORAMINIFERS	NANNOFOSSILS	RADIOLARIANS	DIATOMS	SECTION	METERS	GRAPHIC LITHOLOGY	DRILLING DISTURBANCE	SEDIMENTARY STRUCTURES	SAMPLES
						1	0.5, 1.0				
						2					
						3					

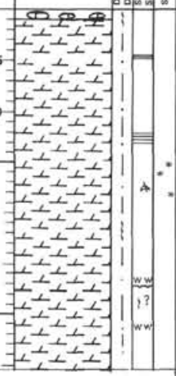

LITHOLOGIC DESCRIPTION

DOLOMITE, variable colors ranging from light yellowish brown (2.5Y 6/4) to grayish brown (2.5Y 5/2), mottled light yellowish brown (2.5Y 6/2) and olive yellow (2.5Y 6/6); more yellowish pieces tend to be more coarser grained than dark grayish brown fragment. Reddish yellow (7.5Y 8/8) staining is common throughout, especially around altered dark, Fe-rich(?) patches. Structures are vaired. Small (1–3 mm) shell molds occur in microporous dolomite between 0–40 cm, Section 2. Pieces at 60 and 78 cm, Section 1, have large (0.5–3.0 mm) flattened pores (fenestral or birds-eye-like porosity). Layering is common but indistinct at several levels: 120–130 cm, Section 1, and 108–112 cm, Section 2. Latter are thin, wavy or crinkled; one is broken with upturned ends (mudcracks?). Small (0–2 cm) laminated, pale yellow (2.5Y 7/4) dolomite fragment or void fill is included in darker dolomite at 48 cm, Section 1. Mottled breccias consisting of darker finely crystalline broken dolomite fragments in fine to coarser dolomite occurs at 144–150 cm, Section 1 and 132–144 cm, Section 2. Latter appears to consist of less broken, darker, finely crystalline dolomite going down in that interval. Both breccias are dolomitized and fabric is relict. Somewhat similar "nodular"-like or brecciated dolomite (relict fabric) occurs at 15–30 cm, Section 3. Last 25 cm of core is coarse grained olive yellow massive dolomite with even coarser-grained, burrow-like zones or patches near the base. Several white (N9) limestone fragments with skeletal debris occur at top of core (0–13 cm).

Thin Sections:

2, 7: Dolomite – interlocking 4–40 μm rhombic crystals of dolomite with dark irregular seams of fine-grained material (organic matter?) along crystal contacts. Scattered 0.5–1.0 mm micropores.

2, 14: Dolomite – as in Section 2, 7 cm but with several 0.1 mm long peloids composed of very finely crystalline dolomite sparsely distributed.

2, 34: Dolomite – as in Section 2, 7 cm but with some yellowish staining of crystals especially near pores and along crystal boundaries. One 5 mm thick zone of very high porosity. Porous~0.2 mm+ across.

SITE 536 HOLE CORE 23 CORED INTERVAL 203.5–213.0 m

TIME – ROCK UNIT	BIOSTRATIGRAPHIC ZONE	FOSSIL CHARACTER: FORAMINIFERS	NANNOFOSSILS	RADIOLARIANS	DIATOMS	SECTION	METERS	GRAPHIC LITHOLOGY	DRILLING DISTURBANCE	SEDIMENTARY STRUCTURES	SAMPLES
						1	0.5, 1.0				
						2					
						3					
						4					

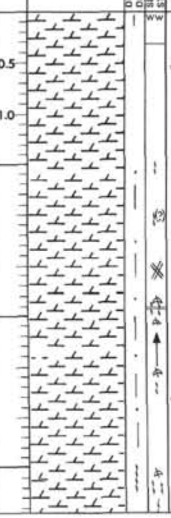

LITHOLOGIC DESCRIPTION

DOLOMITE, color is variable from light yellowish brown (2.5Y 6/4) to grayish brown (2.5Y 5/2), olive yellow (2.5Y 6/6), moderate yellowish brown (10YR 5/4), dark yellowish brown (10YR 4/2), and dark yellowish orange (10YR 6/6). Structures and textures also variable. Abundant thin skeletal molds in parts (e.g. Section 2, 120–130 cm; Section 3, 0–10 cm, and Section 4, 0–25 cm). Some thin crinkly layering in Section 1 at 0–15 cm and indistinct layering at 130–140 cm, Section 2. Possible burrows as marked. Coarsely crystalline olive yellow dolomite at 50–75 cm in Section 2 has common, round (1–2 cm), darker and indistinct spots or blotches. Finely crystalline interval with complex surface below this at 80–87 cm, Section 2. Large open pores or vugs at 70–80 cm Section 2. Below this at 80–102 cm, dolomite is porous with common lighter angular fragments up to 3 mm long – appears to be a breccia. Some manganese staining. Reddish yellow (7.5YR 6/6) iron-stains throughout core.

Thin Sections:

1, 58: Dolomite – interlocking rhombic crystals of dolomite ~5–50 μm across with dark material at some intercrystal boundaries. Several scattered quartz(?) silt-size grains. Porosity is moderate, formed by 0.2–2.0 mm irregular vugs.

2, 86: Dolomite – as at Section 1, 58 cm but with variations in crystal-size that suggest large shell fragments may have been present; some circular patches of coarser dolomite aligned in accurate fashion suggests intraskeletal cementation.

3, 88: Dolomite – as at Section 2, 86 cm. Perhaps up to 10% clay. Porosity 2% voids.

SITE 536 HOLE A CORE 1 CORED INTERVAL 0.0–7.5 m

TIME-ROCK UNIT	BIOSTRATIGRAPHIC ZONE	FORAMINIFERS	NANNOFOSSILS	RADIOLARIANS	DIATOMS	SECTION	METERS
late Pleistocene–Holocene	*Emiliania huxleyi* CN15		AG, AG, AG, AG			1, 2	0.5, 1.0
late Miocene	*Amaurolithus primus* CN9b		AG, AG			2, 3	
late Oligocene	*Cyclicargolithus floridanus* CP9a *Globigerina opima* P21b		AG	AG		3, 4, 5, CC	

GRAPHIC LITHOLOGY / DRILLING DISTURBANCE / SEDIMENTARY STRUCTURES / SAMPLES

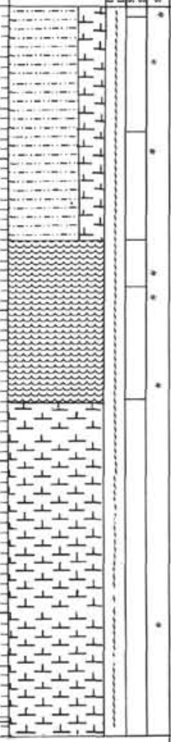

LITHOLOGIC DESCRIPTION

NANNOFOSSIL MUD, MARL, and OOZE MUD is moderate yellowish brown (10YR 5/4) to light brownish gray, light olive gray (5Y 6/1) and gray (10YR 6/1–10YR 5/1) with some sharp boundaries between colors. Some mottling of darker colors in mud. Marl is light greenish gray (5GY 8/1) between 80–125 cm Section 2, then light olive gray (5Y 5/2) to pale olive (10Y 6/2) below. Both are mottled with some glauconite and pyrite (?). Base of Section 3 and Sections 4 and 5 are white (2.5Y 8/0) ooze part of which is semi-lithified. It is structureless except for some drilling injections of brown ooze in Section 5. Pteropods common in top of Section 1. Intense drilling deformation.

SMEAR SLIDE SUMMARY (%):

	1, 5 M	1, 54 D	1, 142 M	2, 75 M
Texture:				
Sand	20	4	1	25
Silt	60	56	67	53
Clay	20	40	32	22
Composition:				
Quartz	–	3	–	–
Mica	20	10	1	3
Clay	20	40	67	22
Volcanic glass	10	–	5	–
Carbonate unspec.	5	10	5	5
Foraminifers	20	1	1	25
Calc. nannofossils	13	30	20	45
Diatoms	10	–	–	–
Radiolarians	–	5	1	–
Sponge spicules	2	–	–	–
Tunicate and holothurian spicules	Tr	–	–	–
Pteropods	3	–	–	–
Dolomite	–	–	–	–

	2, 116 M	2, 138 M	3, 75 D	5, 11 D
Texture:				
Sand	5	5	–	2
Silt	65	65	80	88
Clay	30	30	20	10
Composition:				
Quartz	–	–	–	–
Mica	5	–	–	–
Clay	30	30	20	10
Volcanic glass	–	–	–	–
Carbonate unspec.	5	12	10	5
Foraminifers	5	5	Tr	2
Calc. nannofossils	60	63	70	83
Diatoms	–	–	–	–
Radiolarians	–	–	–	–
Sponge spicules	–	–	–	–
Tunicate and holothurian spicules	–	–	–	–
Pteropods	–	–	–	–
Dolomite	–	Tr	–	–

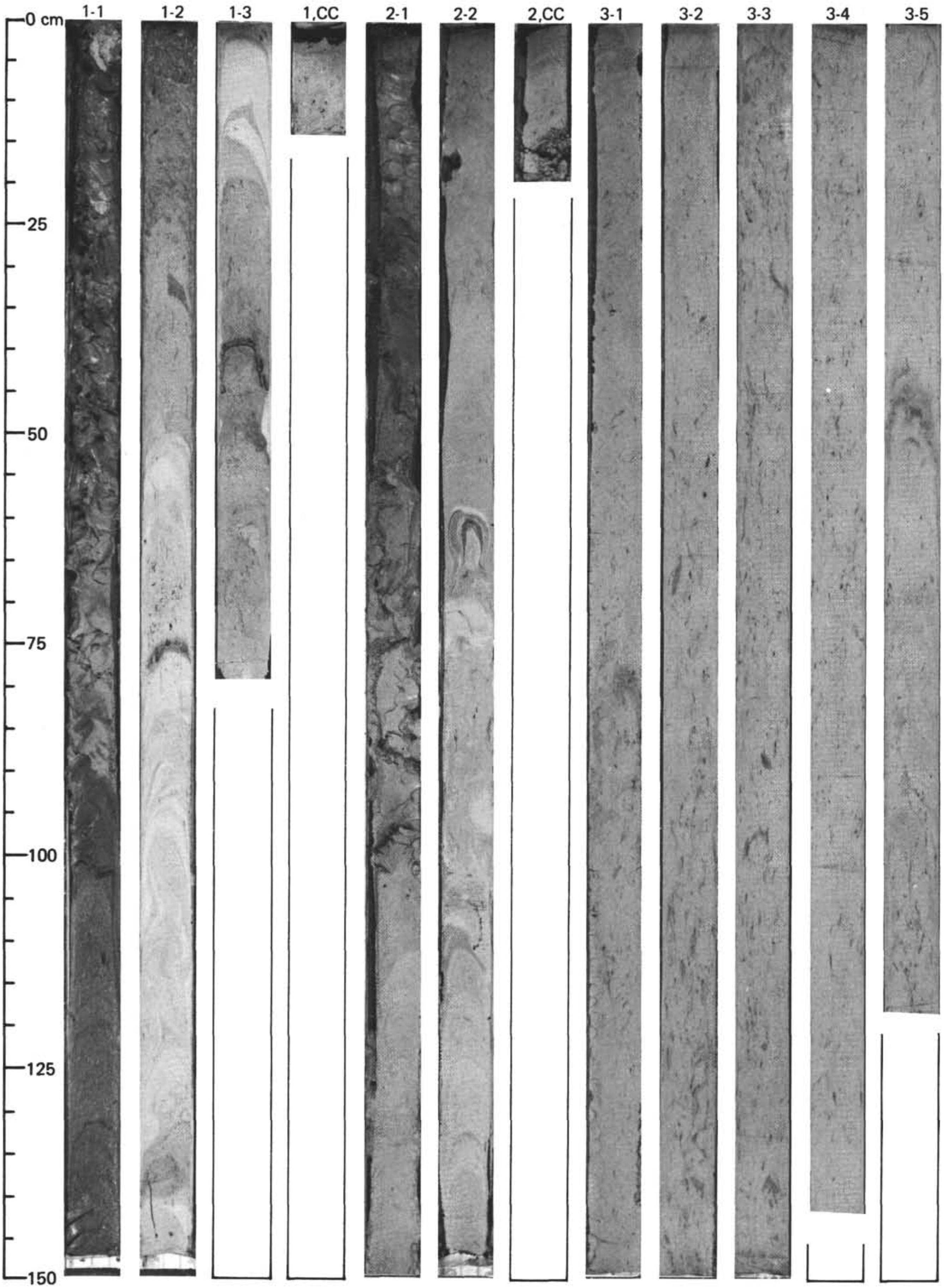
0 cm
25
50
75
100
125
150
1-1
1-2
1-3
1,CC
2-1
2-2
2,CC
3-1
3-2
3-3
3-4
3-5

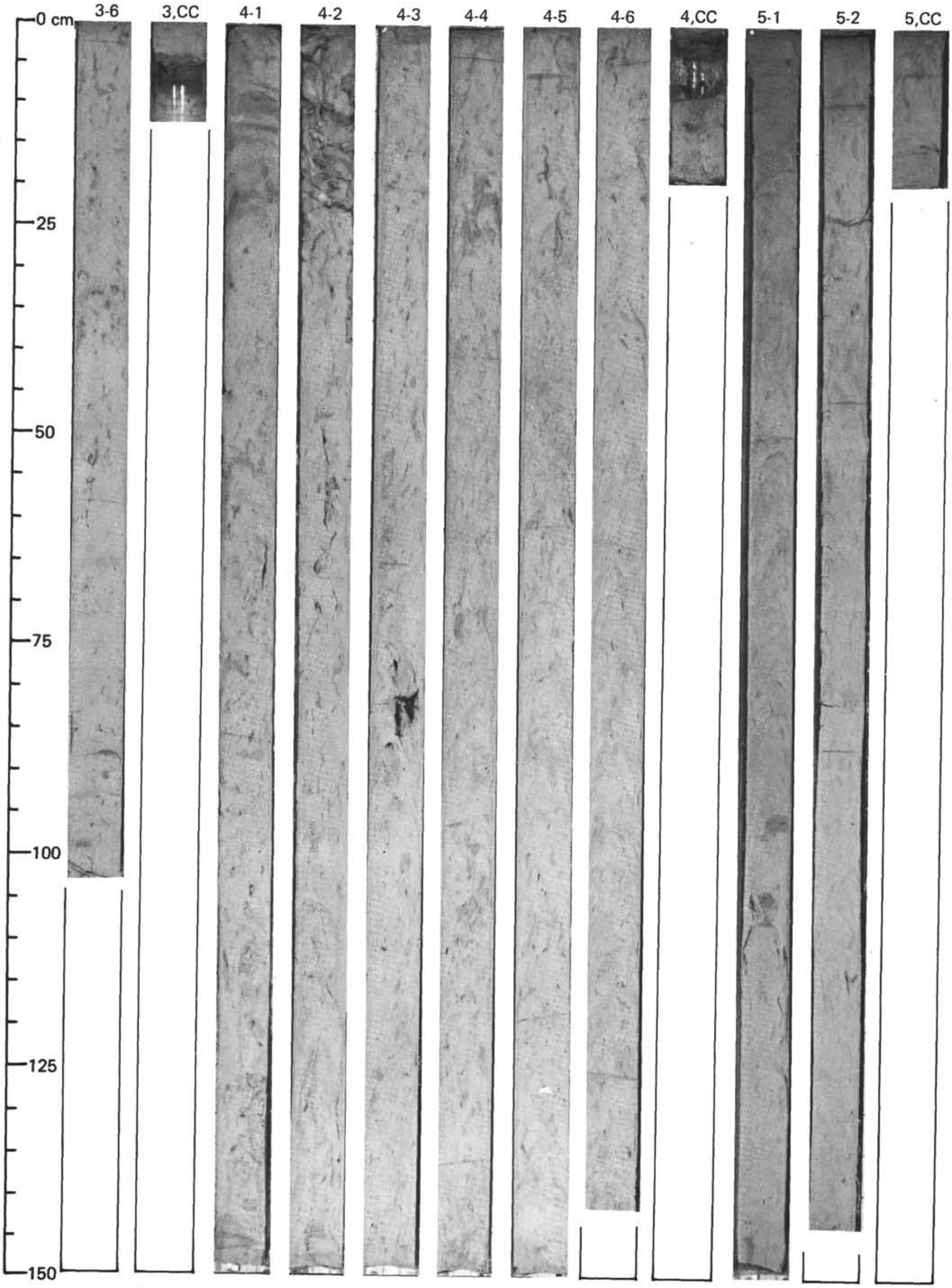
0 cm
25
50
75
100
125
150
3-6
3,CC
4-1
4-2
4-3
4-4
4-5
4-6
4,CC
5-1
5-2
5,CC

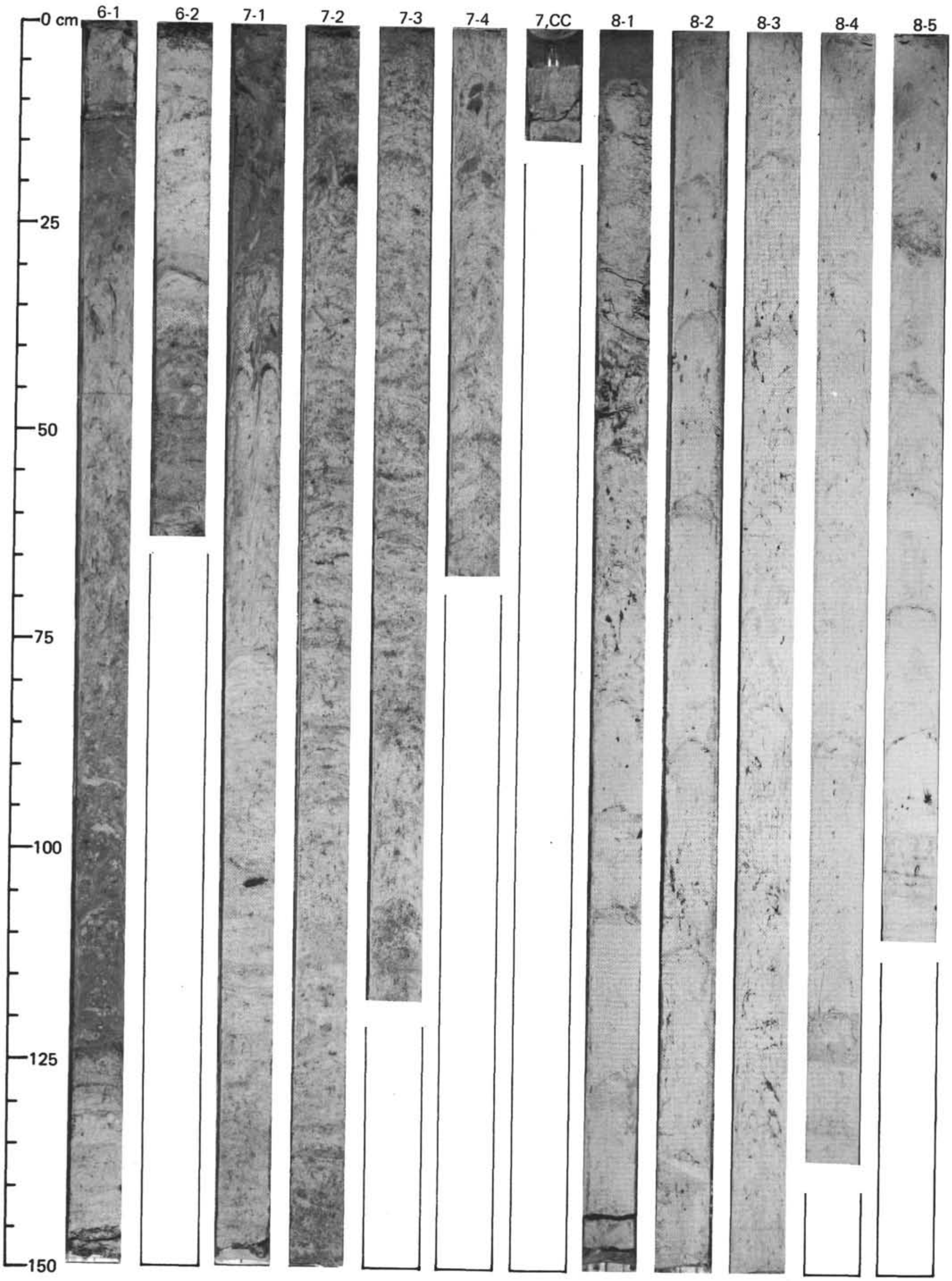
0 cm
25
50
75
100
125
150
6-1
6-2
7-1
7-2
7-3
7-4
7,CC
8-1
8-2
8-3
8-4
8-5

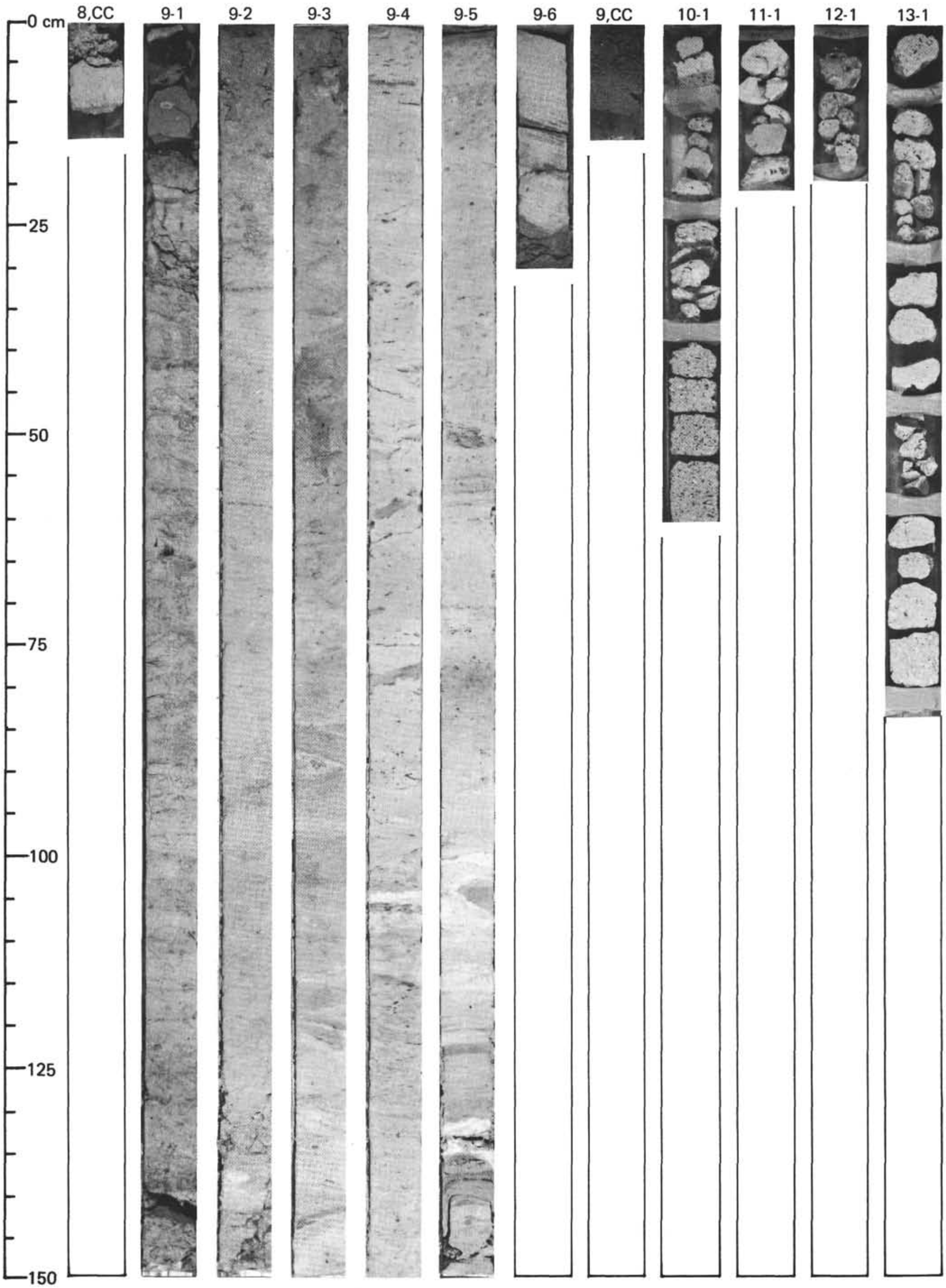
0 cm
25
50
75
100
125
150
8,CC
9-1
9-2
9-3
9-4
9-5
9-6
9,CC
10-1
11-1
12-1
13-1

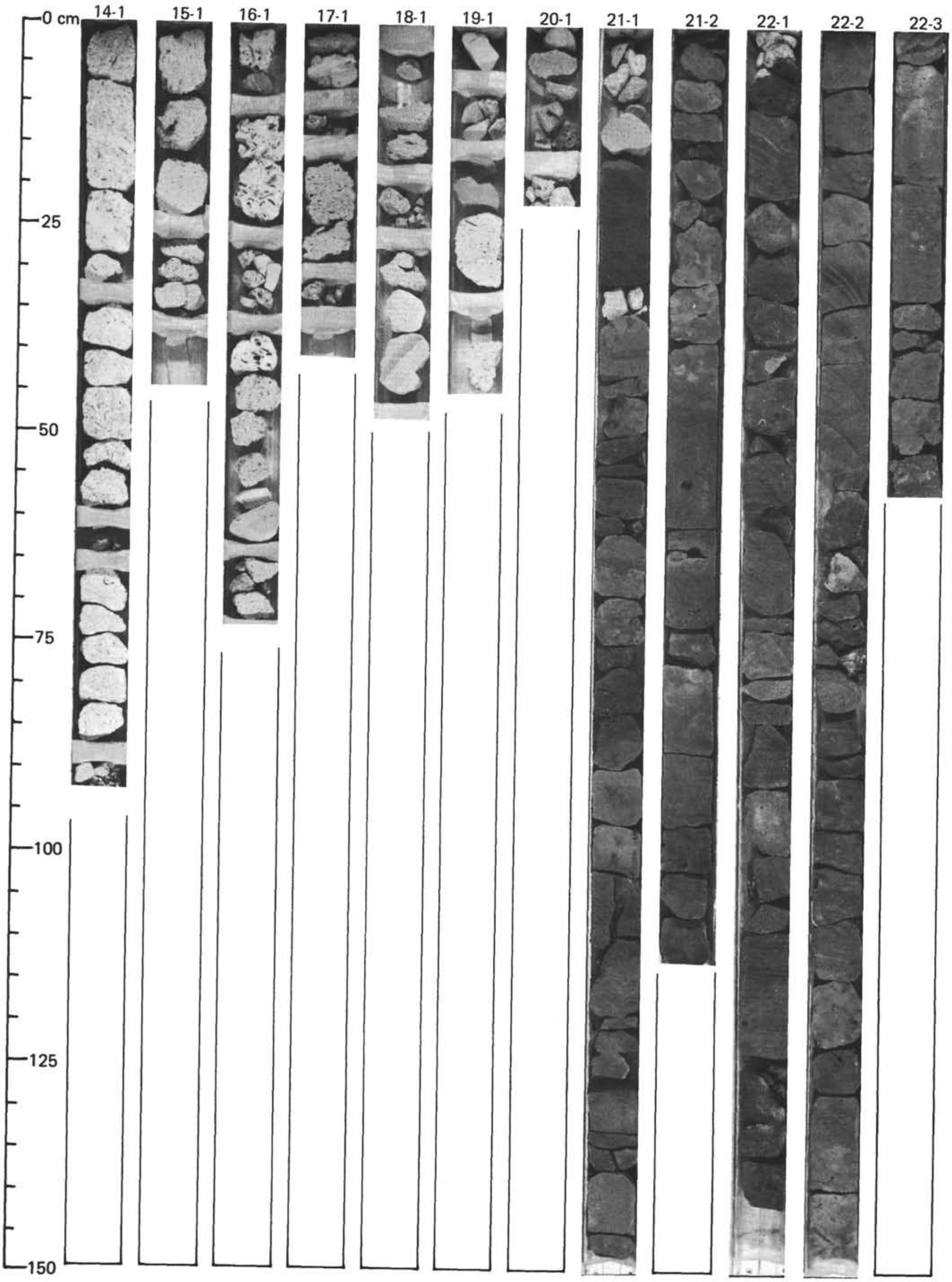
0 cm
25
50
75
100
125
150
14-1
15-1
16-1
17-1
18-1
19-1
20-1
21-1
21-2
22-1
22-2
22-3

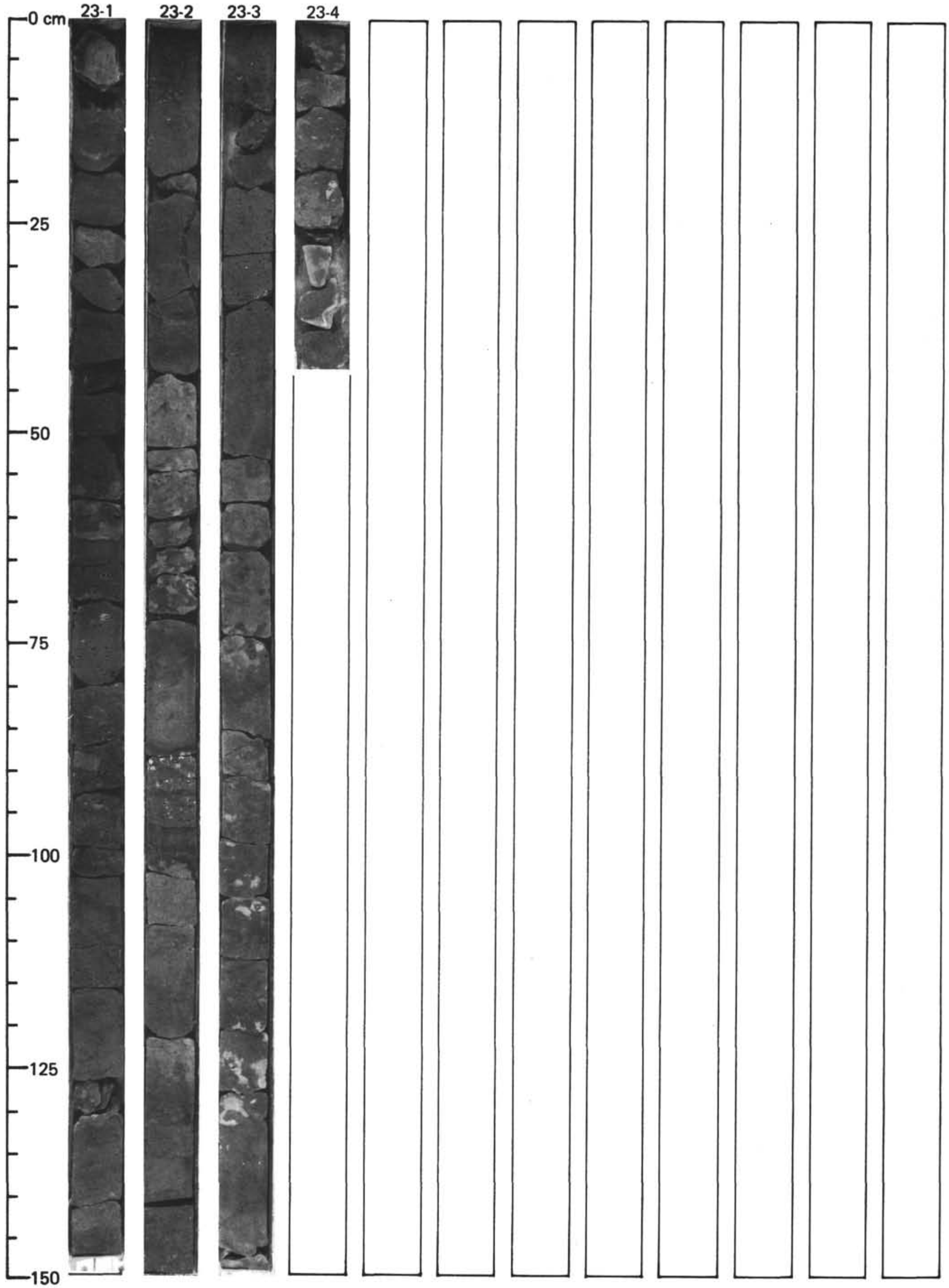
0 cm
25
50
75
100
125
150
23-1
23-2
23-3
23-4